AFOSR - TR - 72 - 1159

FINAL REPORT

TRANSPORT AND STABILITY OF A VORTEX WAKE

by

I. H. Tombach

Principal Investigator

to

Director of Aeromechanics and Energetics
Air Force Office of Scientific Research
ATTN: NAM
Arlington, Virginia 22209

Contract No. F44620-70-C-0032

17 April 1972

Meteorology Research, Inc.
464 West Woodbury Road
Altadena, California 91001

MRI 72 FR-1010

75

FINAL REPORT

TRANSPORT AND STABILITY OF A VORTEX WAKE

by

I. H. Tombach

Principal Investigator

to

Director of Aeromechanics and Energetics
Air Force Office of Scientific Research
ATTN: NAM
Arlington, Virginia 22209

Contract No. F44620-70-C-0032

17 April 1972

Meteorology Research, Inc.
464 West Woodbury Road
Altadena, California 91001

MRI 72 FR-1010

UNCLASSIFIED

Security Classification

DOCUMENT CONTROL DATA - R & D

(Security classification of title, body of abstract and indexing annotation must be entered when the overall report is classified)

1. ORIGINATING ACTIVITY (Corporate author) METEOROLOGY RESEARCH, INC. 464 WEST WOODBURY ROAD ALTADENA, CALIFORNIA 91001	2a. REPORT SECURITY CLASSIFICATION UNCLASSIFIED 2b. GROUP

3. REPORT TITLE

TRANSPORT AND STABILITY OF A VORTEX WAKE

4. DESCRIPTIVE NOTES (Type of report and inclusive dates)

Scientific Final

5. AUTHOR(S) (First name, middle initial, last name)

IVAR H TOMBACH

6. REPORT DATE	7a. TOTAL NO. OF PAGES	7b. NO. OF REFS
17 April 1972	71	58

8a. CONTRACT OR GRANT NO F44620-70-C-0032	9a. ORIGINATOR'S REPORT NUMBER(S) MRI 72 FR-1010
b. PROJECT NO. 9781-02	
c. 61102F	9b. OTHER REPORT NO(S) (Any other numbers that may be assigned this report) AFOSR - TR - 72 - 1159
d. 681307	

10. DISTRIBUTION STATEMENT

Approved for public release; distribution unlimited.

11. SUPPLEMENTARY NOTES TECH, OTHER	12. SPONSORING MILITARY ACTIVITY AF Office of Scientific Research (NAM) 1400 Wilson Boulevard Arlington, Virginia 22209

13. ABSTRACT

The influence of the atmospheric environment on the transport and decay of a trailing vortex wake has been studied analytically and experimentally during a two-year long research program. An analytical model describing the descending motion of an entraining wake in a stably stratified atmosphere has been developed. This model was compared with several other recent theoretical analyses and with limited experimental observations in order to determine the validity. As a consequence of the poor understanding of the details of entrainment and a lack of experimental data, no one model can be judged to be wholly satisfactory (although some appear to describe observed behavior better than others). A flight test program was carried out in which the smoke-marked vortices behind a lightplane were observed in an atmosphere of measured turbulence and stratification. The wake was observed to decay from both sinuous and bursting type instabilities, and the lifetime of the wake was correlated with the level of atmospheric turbulence and the degree of atmospheric stability. Turbulence was found to have a strong effect on wake life, regardless of the mode of decay, with the atmospheric stratification having a weaker influence. The descending motion of the wake was also measured, as was the vortex spacing during the descent. One exceptionally long-lived vortex was observed. The results of these tests were compared with those of some small-scale model experiments and of some large aircraft flight tests.

DD FORM 1 NOV 65 1473

UNCLASSIFIED

Security Classification

UNCLASSIFIED

Security Classification

14 KEY WORDS	LINK A		LINK B		LINK C	
	ROLE	WT	ROLE	WT	ROLE	WT
WAKE TURBULENCE						
TRAILING VORTICES						

UNCLASSIFIED

Security Classification

TABLE OF CONTENTS

1 INTRODUCTION

The trailing vortices generated by a lifting surface moving through the air are left behind in a complex environment. The atmosphere is stratified vertically, since its density, temperature, and pressure vary with altitude. If this stratification is stable, then vertical motions are inhibited, while unstable stratification enhances vertical atmospheric mixing and results in turbulence. Unstable stratification is not a prerequisite for the presence of atmospheric turbulence, however, since wind shear or air flow around obstacles can result in turbulence in even the most stably stratified atmosphere. The atmospheric environment also moves laterally (wind) and vertically (thermals, updrafts, downdrafts) with various scales of motion.

Since the energy present in the atmosphere is so very great, at some point in the life of even the most energetic trailing vortex system the atmospheric factors will begin to influence and eventually dominate its motion and decay. In order to better understand some of these interactions between aircraft wakes and the atmosphere, the Air Force Office of Scientific Research has supported the research program which is presented in this report. This two-year theoretical and experimental study investigated the influence of atmospheric stratification and turbulence on the trailing vortex pair.

The problem was approached in two ways. First, a model was formulated, using integral properties of the wake, to try to understand the influence of atmospheric stratification on the descending motion of the wake. Second, a field investigation of the motion and decay of trailing vortices generated by a lightplane in measured atmospheres was carried out. The results of these endeavors are presented in the following sections.

2. THEORETICAL STUDY OF WAKE TRANSPORT IN A STABLY STRATIFIED ATMOSPHERE

In order to obtain some understanding of the dominant influences of atmospheric stability on the motion of a descending vortex system, the first part of the research program was devoted to the development of a simple analytical model of the wake. Since details of this model have been published (Tombach, 1971), the discussion below will review the important points of that work and will present work which has been carried out since that time. A copy of the full theoretical formulation is included as Appendix A.

2.1 The Model

The model treats the wake as an idealized pair of parallel contra-rotating vortices surrounded by an oval cylinder of accompanying fluid. This two-dimensional system, which is similar to the classical potential flow model, is allowed to descend through a stably stratified, compressible atmosphere. The wake becomes buoyant as it descends because its density increases at a slower (adiabatic) rate than the ambient density. The buoyancy thus generated acts to decrease the wake momentum and circulation, while entrainment of the denser ambient air acts to decrease the buoyancy.

Three assumptions were made to make the problem tractable. First, geometric similarity was assumed so that the size of the wake oval was assumed to scale with the vortex spacing. This constrains the oval to a constant height-to-width ratio, which limits the applicability of the solution to cases where the oval height is sufficiently small so that wake collapse due to gravity is not a factor. The second assumption is that the overall entrainment and mixing process can be characterized by a single parameter which can be represented as a length in the Bjerknes circulation equation, with the rate of change of the circulation of one vortex proportional to this length. The third assumption is that this length also scales with all the other lengths, which then results in this rate of change of circulation being related to the wake scale and the atmospheric stability, and suppresses any explicit display of the effect of the wake buoyancy. Although a similar assumption was used by Turner (1960) and is supported by experiments by Woodward (1959) with thermals, it is not a valid one to make initially when the vortex wake has no buoyancy and thus is not generating any vorticity. (A way to remove this limitation will be presented later.)

Thus the transport model, as presented in Appendix A, does not properly describe either the initial behavior of the wake nor can it properly treat wake behavior at very long times. But for the very important intermediate interval, it presents some very illuminating results which are presented below.

2.2 Transport Solutions

The solutions obtained under the above assumptions indicate that two distinct types of wake behavior may be possible, with the choice of which behavior will occur being determined by the initial vortex strength, the atmospheric stability, and the degree and manner of entrainment (which at present cannot be quantified). If the initial vortex strength is weak enough and/or the stability great enough, the buoyancy rapidly erodes the circulation and the residual momentum (or, more properly, impulse, since it includes the vortical motion) can only be accommodated by an increase in the vortex separation and a slowing down of the wake descent. The motion is much like that of a vortex pair descending into ground effect.

On the other hand, if the vortex is strong or the stability weak, then the behavior is quite different. In this case, there is residual circulation remaining when the impulse has been eliminated by the buoyancy, and the kinematical consequence is a rapid convergence of the vortices with an accompanying downward acceleration, resulting in an inevitable destruction of the vortices. The index determining which behavior will occur, denoted by Q, is given by

$$Q \propto \frac{1}{G^{1/2}} \frac{\Gamma_0}{b_0^{2}} \quad (1)$$

where

$$G = \frac{g}{\rho_0} \frac{d\rho}{dz} - \frac{g^2}{a_0^{2}} \quad (2)$$

is the atmospheric density gradient relative to the adiabatic one, Γ_0 is the initial circulation of one vortex, $2b_0$ is the initial vortex spacing, and a_0 is the speed of sound. The proportionality factor (given in Appendix A) depends on the entrainment details.

The time scale of the motion is found to be proportional to $G^{-1/2}$, hence the greater the stability the more rapidly the motions described above take place. The vertical length scale is proportional to $G^{-1/3}$, hence as the atmospheric stability is increased the vertical extent of the motion will decrease.

Some experimental observations of wake descent have been made and they correlate well qualitatively with the behavior predicted by the model. A study at MRI of the dissemination of particles released from aircraft (Smith and Wolf, 1963; Smith and MacCready, 1963) included some observations of wake descent from a variety of aircraft. Tests with aircraft up to DC-3 size gave typical descent distances of 25 to 100 feet over land, with the wake descending initially at the theoretical speed, but then broadening and slowing up. On the other, similar measurements over the ocean sometimes, but not always, indicated wake descents of 600 feet. The most logical explanation was that turbulence slowed the wake's motion and helped spread it and that a stable atmosphere further impeded descent since the wake acquired buoyancy while moving downward. Both stability and turbulence are usually less over the ocean than over land, thus resulting in longer vortex life and descent.

Another study, the joint FAA-NASA-Boeing flight test study of wakes behind jumbo jet aircraft (FAA Task Force, 1971) found that the vortices began descending at 400 to 500 feet per minute but that fully developed vortices were not found more than 1000 feet below the altitude of the generating aircraft. Leveling off, combined with start of breakup, usually began after a descent of 800 to 900 feet. The vortex spacing appeared to remain constant until breakup; very little attenuation of vortex strength was observed prior to breakup (i.e., prior to two minutes age). In contrast, during a British study of wakes behind jet transport aircraft (Rose and Dee, 1965), wake descents of up to 800 feet were measured during the first 150 seconds of wake life and no general leveling-off trend was observed.

The only known quantitative measurements of vortex spacing were obtained in another British study (Bisgood, et al., 1971) where the vortex spacing behind a delta-wing aircraft was observed to grow to about three times the initial spacing in about 45 seconds. A similar result has been observed by the author, where a contrail-marked wake behind a jet transport was observed to more than double its vortex spacing in about one minute.

The motion of wake vortices was also measured in the current flight test program and the results agree qualitatively with those above, although an additional factor affecting wake descent was discovered. A detailed discussion of these results follows in Section 3.

Some observations of transport aircraft wakes also seem to indicate that the wake sometimes oscillates vertically about the final level.

The present solution is unable to treat such behavior because the motion always terminates in a singularity of the solution which prevents a reversal of the wake descent, except for the unique case of $Q = \pi/2$ (discussed in Appendix A). This unreal singularity comes about from the coupling of the circulation change to the wake scale, which is no longer valid when the wake can no longer be assumed to be geometrically similar to its original state. As will be pointed out later, an oscillatory motion of the wake would be one which is dominated by the stratification rather than by the vortex dynamics, and it is thus likely that such a wake would have suffered a collapse and would consequently bear little resemblance to the configuration assumed for the model.

The observations do tend to suggest that the first (weak vortex/strong stability) solution, characterized by a slowing down or stopping of descent and, possibly, an increase in the vortex spacing, is a common wake behavior. This also seems likely from study of the model, since the second form of solution, in which the vortex spacing decreases, might be expected to be unstable and to have a relatively brief lifetime since the convergence of the vortices both increases the interaction between the vortices and requires the detrainment of fluid mass (and the vorticity contained therein) from the wake oval.

2.3 Implications for Decay

The transport model discussed above provides some clues as to which combinations of wake characteristics and atmospheric properties might tend to result in an unstable wake configuration. As was stated earlier, one of the solutions of the model equation results in a vortex system which must lose mass as it descends. It is unlikely that such a process of detrainment can continue for long in any organized manner* and consequently such wakes are probably very short lived.

The conclusions to be derived about wake stability from this interpretation of the model are at best tentative, but are interesting enough to warrant consideration. One portion of the solution, corresponding to relatively strong atmospheric stability and weak circulation is completely stable from the entrainment related instability point of view. On the other hand, the other half of the solution, corresponding to a strong circulation and weak stability combination is always unstable. The lifetime of the ordered motion in this region apparently varies only weakly with changes in circulation but increases quite rapidly as the stability is

*Although Scorer and Davenport (1970), in a model to be discussed below, demonstrate one detrainment mechanism which could postpone the inevitable wake destruction for a short while.

decreased. The conclusion reached is thus that, given a fixed vortex strength, the wake lifetime is long when the atmospheric stability is nearly neutral (but stable), it reaches a minimum at some increased level of stability, and then again increases when the environmental stability is sufficiently great to cause the vortex spacing to increase. Very limited observations of actual wakes suggest that long lifetimes at neutral and strong stabilities do prevail, but the suggestion that there is a point of minumum lifetime in between is intriguing.

The stability of the wake is not solely dependent on whether or not detrainment takes place, of course, and other considerations may well dominate the wake behavior. One important factor is the generation of vorticity at the wake upper surface as a consequence of the buoyancy. This vorticity, which is opposite in sign to that in the vortex, results in an instability according to the stability criterion of Rayleigh, which states that any inviscid flow in which the circulation decreases with increasing distance from the axis is unstable. The model proposed by Scorer and Davenport shows one way in which this reverse vorticity can be detrained from the wake so as to delay the onset of this hydrodynamic instability.

A very strong destructive influence on the wake is the sinusoidal interaction of the two vortices with each other, resulting eventually in the formation of a trail of vortex rings in place of the parallel vortex pair, as shown for the contrail-marked vortices in Fig. 1. A theory by Crow (1970) describes this phenomenon by considering only the mutual- and self-induction of a slightly perturbed vortex pair. Since his model appears to adequately describe the motion, he states that buoyancy is probably not an essential mechanism for this instability, contrary to the opinion of Scorer (1958) and Scorer and Davenport (1971). This point will be discussed further in the description of the experimental portion of the current program.

The distance separating the vortices plays a key role in the growth of this instability since Crow calculates its amplification time constant to be proportional to b^2. Consequently, such sinuous instabilities grow much more rapidly when the vortices are closer together, which again forecasts a short lifetime for the strong vortex/weak stability solution of the present model.

2.4 Comparison with Other Theories and Some Experiments

In the last several years, a number of theories have been created to describe the motion of a vortex pair in a stratified environment. These will be briefly reviewed here.

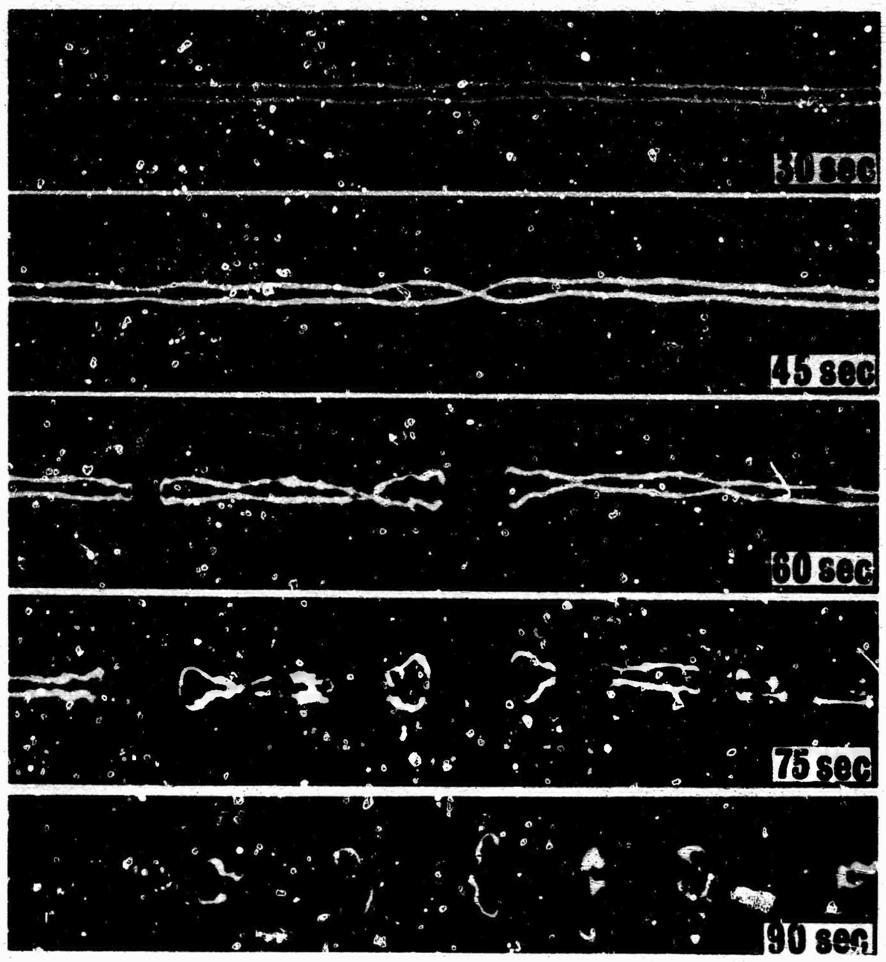

Fig. 1. B-47 CONTRAIL BREAKUP BY SINUOUS INTERACTION OF VORTICES (from Smith and Diamond, 1956, as reproduced by MacCready, 1971)

One theory (Scorer and Davenport, 1970) was published at about the same time as the present theory was presented at the BSRL-AFOSR Symposium on Wake Turbulence in 1970, and is in many ways very similar to it. Scorer and Davenport approach the problem in the same way as the present model, except that they require that the circulation of the vortex system remain constant and thus avoid the need for an assumption about entrainment. They find a single solution in which the vortices converge and accelerate downward in a stable atmosphere, as in the second solution of the present analysis. They compute numerically the internal streamline patterns for this case and suggest that the detrainment is indeed a stable process and that the circulation is, in fact, constant because the vorticity generated by the buoyancy at the boundary of the wake oval is continually detrained. After a time, however, they state that some of this fluid and vorticity is mixed into the wake, which results in its eventual destabilization and destruction. They suggest that the destruction of the vortices occurs in the form of bursts caused by the rapid rise in the central vortex pressure as mixing occurs.

In their model, the sinuous instability of the wake and the subsequent segmentation of the wake into ring-like sections comes about as a consequence of localized manifestations of the proposed descent mechanism, where portions of the vortices descend, converge, and finally burst, leaving behind a segmented vortex trail. The observations by Smith and Beesmer (1959) disagree with this point, indicating instead that the vortex cores make contact, the trail breaks, and is gathered up into rings as shown in detail in Fig. 2. There is no indication of a burst taking place at the point of contact, an observation which was also borne out by the experiments for the present study.

Since both the Scorer and Davenport and Crow models specify that the vortices move locally downward and make contact at their lowest points, which agrees with the experimental observations of Smith and Beesmer and of the present study, the question of whether the sinuous instability is purely a kinematical one or whether atmospheric stability plays a key role cannot be settled here.

Some features of the Scorer and Davenport model are difficult to correlate with observations of wakes. For example, wakes have been observed to level off, yet their mechanism has no point at which the vortices stop descending until the organized motion has been destroyed. On the other hand, photographs of contrails made from the side (Smith and Beesmer, 1959) show a curtain of condensed vapor extending above the wake up to the flight level of the generating aircraft. Qualitatively,

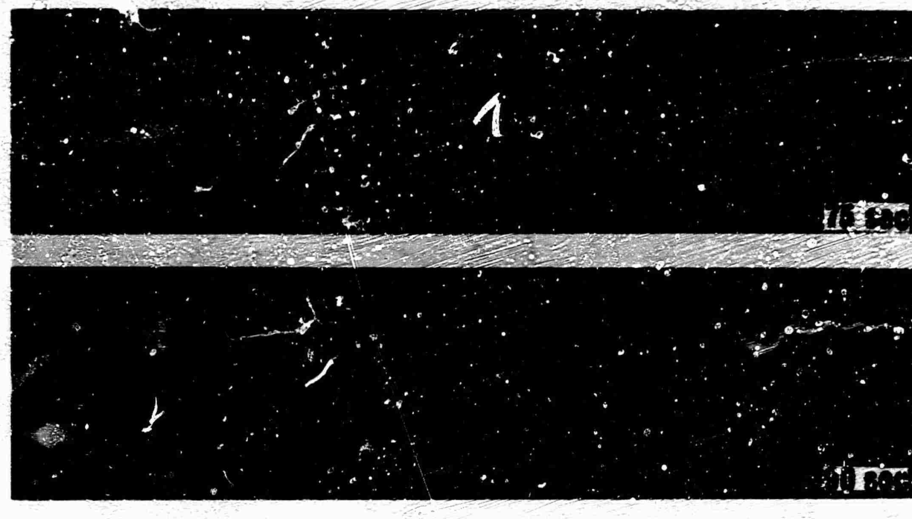

Fig. 2. DETAIL OF B-47 CONTRAIL BREAKUP

this veil appears very much like the sheet of detrained fluid which the Scorer and Davenport model contains, although it is also possible that it may result from material not originally included in the oval cylinder of fluid which accompanies the vortices. These same contrail observations, as well as low altitude measurements by Smith and MacCready (1963), suggest however that the vortex separation increases at least slightly as the wake descends, in a manner more like that in the first solution of the present analysis.

A second theory was developed by Tulin and Shwartz (1971) in which they modeled the vortex system by separate velocity scaling of the flows internal and external to the wake oval with a shear layer at the boundary between the two flow fields (Fig. 3). Based on experiments they performed in a water tank, they conclude that the wake entrains the vorticity generated at this shear layer (in contrast to the detrainment postulated by Scorer and Davenport) but that the ingested vorticity is mainly canceled out at the wake centerline through mixing with vorticity of the opposite sign from the other side of the wake. Consequently, they model a turbulent wake in a stratified medium by assuming conservation of volume, mass, and energy and neglecting vorticity and momentum. They then find completely similar solutions which depend on four parameters — the initial buoyancy of the wake, the stability of the fluid, the dissipation of kinetic energy, and the ratio of kinetic to potential energy. The latter two parameters are assigned values based on their experiments.

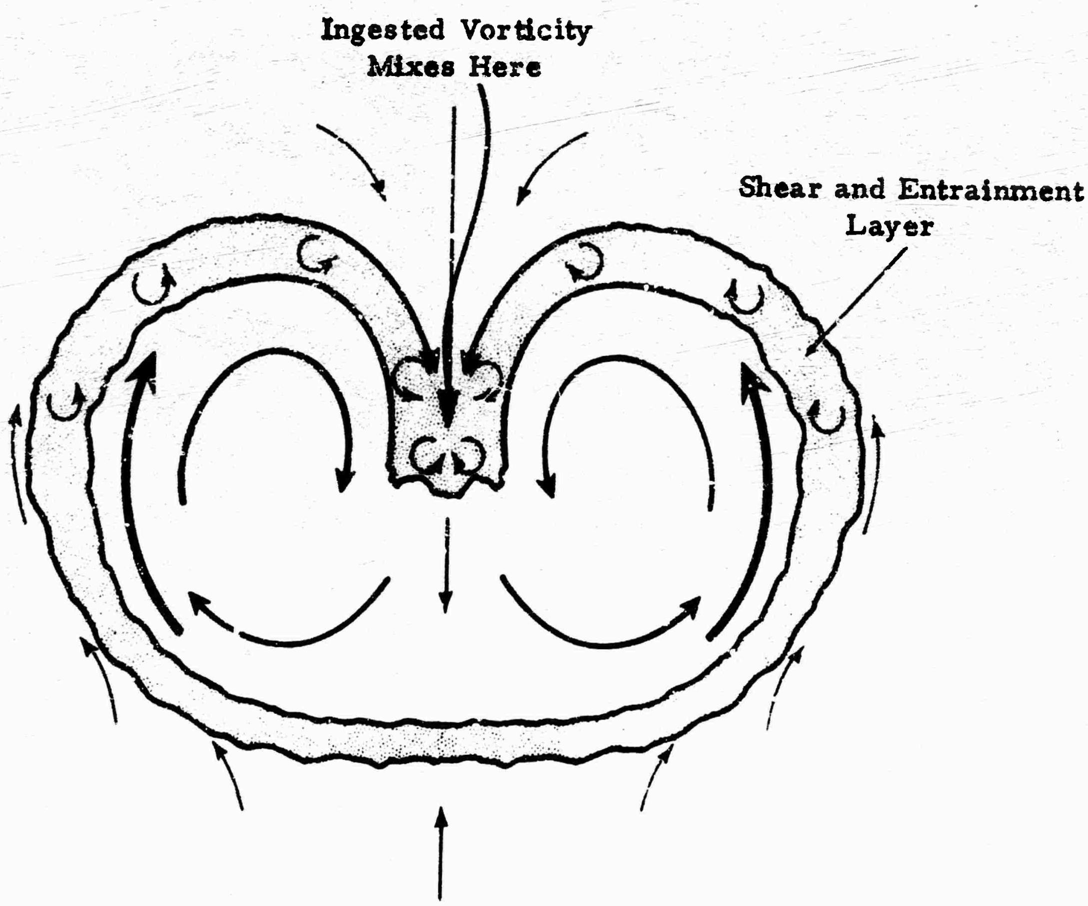

Fig. 3. MODEL OF ENTRAINING VORTEX PAIR USED BY TULIN AND SHWARTZ

Tulin and Shwartz give formulas for vortex wake motion in a stratified medium, which are too complex to present here, and present excellent correlations between their formulas and experiments. Their model predicts that a wake will slow down and stop its descent in a stratified fluid and that the vortex separation will increase as the wake descends. The descent in a homogeneous fluid has the behavior $z \sim t^{1/2}$ and $b \sim t^{1/2}$. In a stably stratified fluid, the descent slows down more quickly and the spreading is more rapid, but similarity no longer holds when the wake has come to rest. Figure 4 presents one of their experimental observations of the wake (redrawn to simulate a vortex wake in a stable atmosphere) with sketches of the wake cross section showing its collapse as the stratification eventually dominates wake behavior. This process takes place in a characteristic time

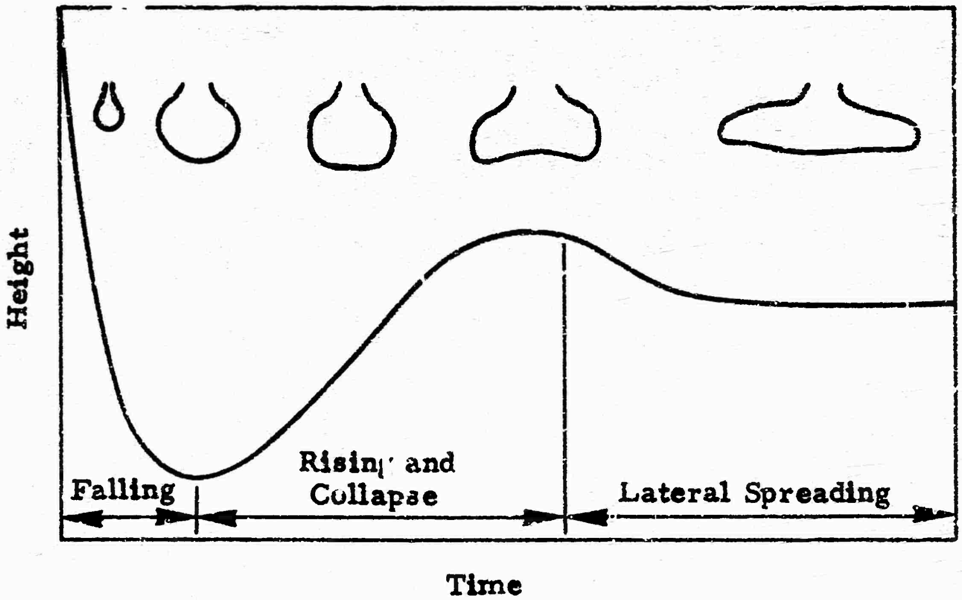

Fig. 4. TRAJECTORY OF A VORTEX PAIR IN A LINEARLY DENSITY STRATIFIED MEDIUM (from Tulin and Shwartz, 1971)

which is proportional to the Väisälä period $T_1 = G^{-1/2}$ (with G defined in Eq. (2)) with the proportionality factor depending on the initial strength of the vortex, represented by another time $T_2 = b/w$, where w is the descent speed of the wake. If $T_2 < T_1$, then the initial wake properties dominate its motion, while if $T_2 > T_1$, then the atmospheric stratification dominates the motion. Since T_2 increases as the wake slows down and grows, stratification will always dominate the motion eventually, unless some instability has first destroyed the wake.

Since, for a given initial vortex configuration, the time scale of the motion is proportional to T_1, then, specifically, the time required for the wake to descend to its maximum level is proportional to T_1. This scaling of time with the stability is a characteristic of motions in the atmosphere and the same relation is present in all three theories presented above, viz., in the model created in the current study as well as in those by Scorer and Davenport and by Tulin and Shwartz.

Saffman (1971) has presented a third model which indicates that a vortex system in a stable environment descends with the vortex spacing remaining constant if there is no entrainment and increasing if entrainment is assumed proportional to the density difference between the wake and environment. In either case, the wake descent is stopped by the stability and it subsequently oscillates vertically. To find these solutions, Saffman solves the Laplace equation for the potentials inside and outside the wake volume, with the constraint that there is no change in wake volume (except due to entrainment, which he treats separately).

As a point of considerable importance, Saffman states that the analyses by Scorer and Davenport and by Kuhn and Nielsen (1972), as well as the present analysis, are in error because they equate the change in the wake impulse (momentum) to the buoyancy force. He notes that this step is correct only if the Boussinesq approximation holds (i.e., if the density difference between the wake and the environment are small) and if all the vorticity generated by the buoyancy is included in the computation of the impulse. He claims that the latter requirement was not satisfied in the analyses in question, and consequently they will give erroneous results.

The criticism is not wholly valid, however. In particular, the present analysis does take into account the change in impulse due to the buoyancy generated vorticity (since the circulation changes according to the Bjerknes equation, Eq. (8) in Appendix A). It does assume, however, that it is possible to approximate the impulse of the wake, including the new vorticity, by the impulse of a geometrically identical wake with all of the vorticity, old and new, concentrated in the two vortex cores. This approximation will probably result in errors after the wake has acquired considerable buoyancy, but by that time the model is no longer valid for a variety of other reasons. Similar comments apply to the criticism of the work by Kuhn and Nielsen, while its validity to the theory of Scorer and Davenport depends on whether or not the detrained vorticity is assumed to be self-annihilating.

The most recent addition to the collection of models of wake transport in a stably stratified environment is one by Kuhn and Nielsen (1972). The approach is the same as that taken by the present analysis and by Scorer and Davenport, except that the entrainment is modeled differently so that part of the buoyancy generated can be entrained and part of it detrained, with the proportions of each being governed by an unknown wake mixing parameter. Their analysis shows the wake accelerates as it descends and the vortex spacing decreases. Increased values of the wake mixing parameter reduce the rates of descent and convergence, while the addition of heated air to the wake, but outside the vortices, is found to cause a leveling-off and spreading of the wake.

One shortcoming of the present model was the assumption that the rate of change of circulation was proportional to the scale of the wake. This is erroneous at small times if the wake has no initial buoyancy, since then one should have no generation of vorticity. Kuhn and Nielsen use a variable entrainment length, proportional to the density difference between the entrained fluid and the ambient fluid, with the entrained fluid density being a weighted average of the ambient density, the density in the vicinity of the vortex, and the density in the region into which the outer fluid is entrained. The effect is to make the parameter s in the present analysis (Eq. (11) in Appendix A) into a variable which has value zero initially.

The behavior of a wake in a stably stratified atmosphere, as predicted by all the various theories, is tabulated in Table 1. There is an obvious lack of agreement, based not only on fundamental questions such as those raised by Saffman but also because of uncertainty about the details of the entrainment process. A good laboratory study of the fate of the buoyancy-generated vorticity seems in order at this point. Based on limited comparisons with experiment, the most likely behavior is that of slowing down and spreading, as was shown in Fig. 4, with at least partial entrainment of vorticity into the wake and annihilation of at least some of the entrained vorticity. Whether, in certain conditions, the converging and accelerating behavior can also be physically realized is not known.

Table 1

COMPARISON OF THEORIES FOR DESCENT OF A VORTEX WAKE IN A STABLY STRATIFIED ATMOSPHERE

	Vortex Spacing	Descent Speed	Buoyancy-Generated Vorticity
Tombach ($\Gamma/G^{1/2}$ small)	Increases	Stops	Entrained
Tombach ($\Gamma/G^{1/2}$ large)	Decreases	Increases	Entrained
Scorer and Davenport (1970)	Decreases	Increases	Detrained
Tulin and Shwartz (1971)	Increases	Stops	Entrained then annihilated on centerline
Saffman (1971)	Increases	Stops	Entrained
Kuhn and Nielsen (1972)	Decreases	Increases	Partly entrained

3. EXPERIMENTAL STUDY OF WAKE TRANSPORT AND DECAY

The second portion of the research program was concerned with the observation of actual trailing vortices in order to better understand their motion and decay, and to measure the impact of atmospheric stability and turbulence on them. The overall philosophy of the field study was that these experiments should be, as nearly as nature would allow, outdoor laboratory experiments in which the parameters of the problem were varied systematically or, if that were not possible, they were measured.

3.1 Description of the Experiments

The experiment plan called for vortex wakes to be generated and marked with smoke in a location where the topography permitted simultaneous photographic observations of the vortices from directly below and from a point level with and to the side of the flight path. Such a location was found near El Mirage Dry Lake in California (Fig. 5) where the Shadow Mountains to the east provided the needed elevated camera platform and a north-south dirt road acted as a tracking aid for the wake generating airplane. One camera installation (Site 1) was located on this road, at an elevation of 875 m (2870 ft). The other camera (Site 2) was situated 1290 m to the east on a lesser peak of the range, at an altitude of 1006 m (3300 ft). The airplane was usually flown southbound along the road at the Site 2 elevation so that it was 131 m (430 ft) above the Site 1 cameras, although various special experiments resulted in variations of this standard pattern.

The wakes were generated by a Cessna 170, a single-engine, high-wing lightplane. The wing span of this aircraft is 11.0 m and its weight (mass) in these experiments was about 910 kg, giving a span loading w/b = 811 newton/m. The circulation about a vortex created by this airplane ranged from $\Gamma = 16\ m^2/s$ up to $33\ m^2/s$ as the forward speed ranged from a high of 56 m/s to a low of 27 m/s. Table 2 summarizes the operating conditions and includes the computed values of circulation and theoretical speed of descent for a vortex pair in potential flow, assuming an elliptic distribution of lift on the wing. All flights were made in level flight with flaps retracted and power set as required to maintain altitude.

The vortices thus generated were marked by colored smoke generated by U. S. Army M-18 smoke grenades which were mounted in specially modified wingtips, as shown in Fig. 6. Four smoke grenades were installed in each wing, with red grenades in the left tip and green ones in the right one. A cable from each tip to the cockpit allowed the grenade pins to be pulled sequentially allowing from 1 to 4

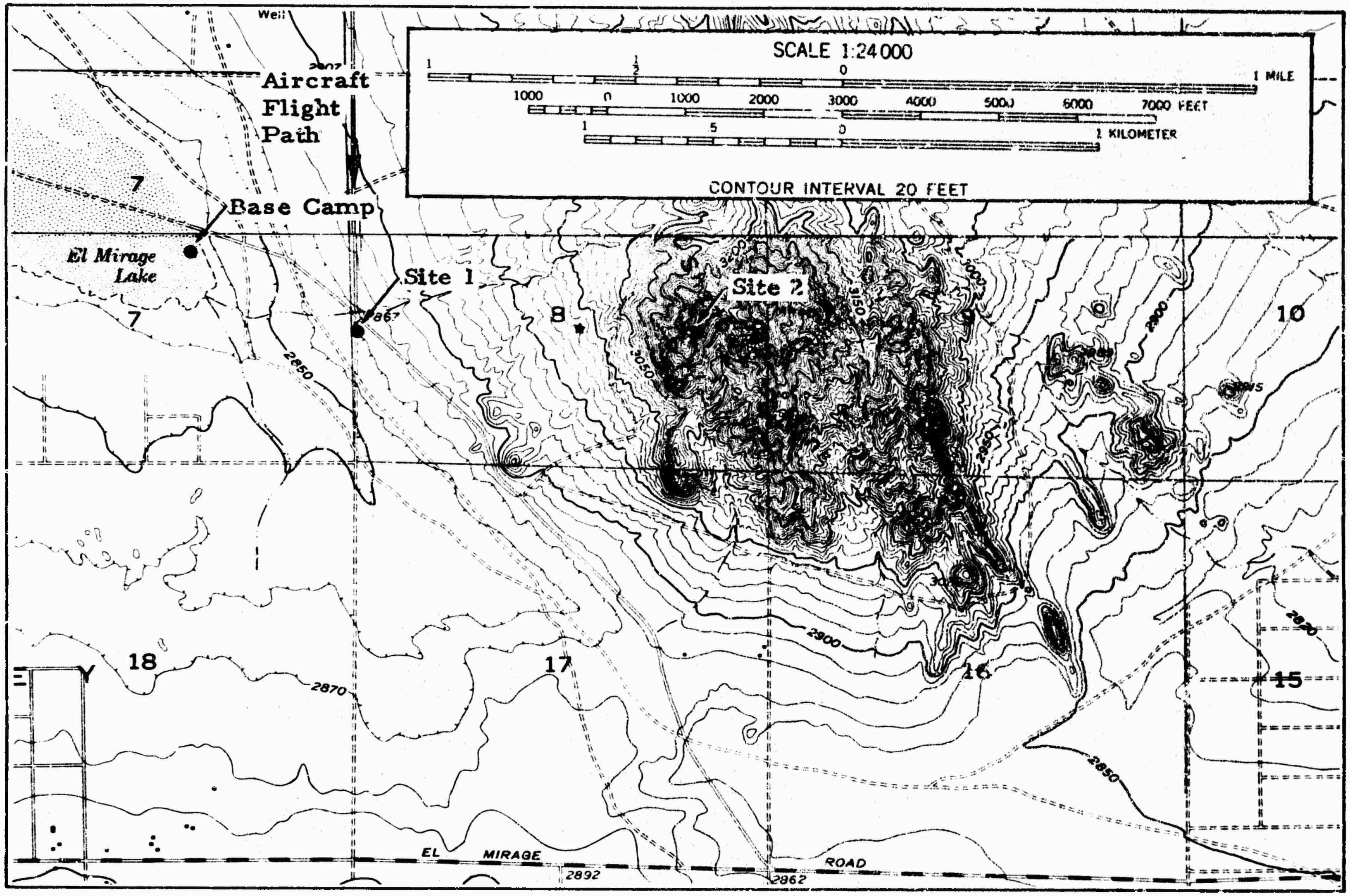

Fig. 5. MAP OF EXPERIMENT SITE.
(The Site 1 location applies for all dates except 5/25, for which the location is marked by * and the flight path is from north to south over it.)

Table 2

TABULATION OF PROPERTIES OF GENERATED WAKES

Date (1971)	Pass No.	V (m/s)	Γ (m^2/s)	w (m/s)
25 May	1-5	33	28	0.52
31 Aug.	1-8	32	29	0.54
3 Nov.	1-4	33	28	0.52
3 Nov.	5	28	33	0.62
3 Nov.	6	58	16	0.30
3 Nov.	7-8	31	30	0.56
4 Nov.	1-8	28	33	0.62

grenades to be used at once on each wing. Some experimentation showed the best photographic quality was obtained when two grenades per vortex were used, which thus allowed the airplane to make two passes past the cameras before it had to land on El Mirage Dry Lake for reloading at the base camp there. Figure 7 shows the residue from the smoke left behind on a wingtip and shows clearly the vortical nature of the airflow over the tip.

In addition to the smoke grenades, instrumentation was also installed on the airplane to measure atmospheric parameters and the aircraft speed and altitude. The air temperature was measured by a thermistor vortex thermometer, pressure altitude with an electrical pressure transducer, airspeed with an electrical differential pressure transducer mounted on a specially installed pitot-static tube, and turbulence was measured with an MRI Universal Indicated Turbulence System (MacCready, 1966) connected to the same differential pressure transducer. All data were recorded on a recorder installed in the aircraft.

By flying soundings near the test area, vertical profiles of turbulence and temperature were determined. The atmospheric stability was then easily determined from the temperature profile. The turbulence was rated in terms of the rate of dissipation of turbulent energy into heat, ϵ, in the inertial subrange of isotropic turbulence (for an explanation of the concept, see MacCready, 1964). The cube root of this quantity

Fig. 6. MODIFIED WINGTIP FOR SMOKE GRENADE INSTALLATION

Fig. 7. SMOKE RESIDUE ON WINGTIP AFTER FLIGHT TESTS

can be related to the "bumpiness" a pilot feels and to the accelerations experienced by him. An experimentally derived correlation between $\epsilon^{1/3}$ and the "feel" was obtained by Gannon, Severson, and Tombach (1970) and will be used below in the presentation of the data from the experiment.

The camera site locations have already been mentioned. Site 1 was equipped with an upward pointing 16-mm motion picture camera on all tests and had a variety of other cameras, as shown in Table 3. On the mountain, Site 2 was outfitted with a horizontally mounted 16-mm camera and, on all but the first test date, a similarly installed 35-mm still camera which took a picture once every 5 seconds. In addition, there was one hand-held 35-mm camera at each site and one in the airplane. Finally, some sequences were filmed with a 16-mm motion picture camera in the aircraft. A photograph of the Site 2 installation appears in Fig. 8.

Several special vehicles were required for the experiment, some of which are shown in Fig. 9. The camper truck served as a combination bunkhouse, chow hall, command post, and equipment van. The sand buggy carried the crew and photographic equipment up the quite steep and sandy slopes of the mountain to Site 2. A trail motorcycle was originally used for the first flight test day on 25 May, but it became mired in the sand and the equipment had to be carried part of the way on foot. The sand buggy was used on all the other test days, except that breakage of its distributor shaft on 3 November resulted in another long uphill hike for the Site 2 crew.

The sequence of events on each experiment day was essentially the same. The field crew arose before sunrise and was in position at the camera sites. The aircraft passes began as soon as there was enough light to photograph the wake and continued until the thermal mixing due to solar heating had eroded the pre-dawn stable stratification and the turbulence level had increased sufficiently to severely shorten the life of the wake. Most passes were flown at the Site 2 elevation along the road shown in Fig. 5, except that all passes on the first test day (25 May 1971) were flown along another road (which is not on the map) which was closer to Site 2. An occasional pass was made at a different altitude or in a different direction to observe the effects of altitude and wind. The aircraft operations were coordinated with activities at the camera sites by radiotelephone units at each location.

Table 3

FIXED CAMERAS USED AT OBSERVATION SITES

Date	Site 1			Site 2		
(1971)	Camera	Lens	Framing Rate	Camera	Lens	Framing Rate
25 May	16 mm	16 mm	12/sec	16 mm	25 mm	24/sec
31 Aug.	16 mm	16 mm	16/sec	16 mm	75 mm	16/sec
	16 mm	10 mm	1/2sec	35 mm	50 mm	1/5sec
3 Nov. &	16 mm	16 mm	16/sec	16 mm	75 mm	16/sec
4 Nov.	35 mm	21 mm	1/6sec	35 mm	105 mm	1/5sec

Fig. 8. SITE 2 CAMERA INSTALLATION

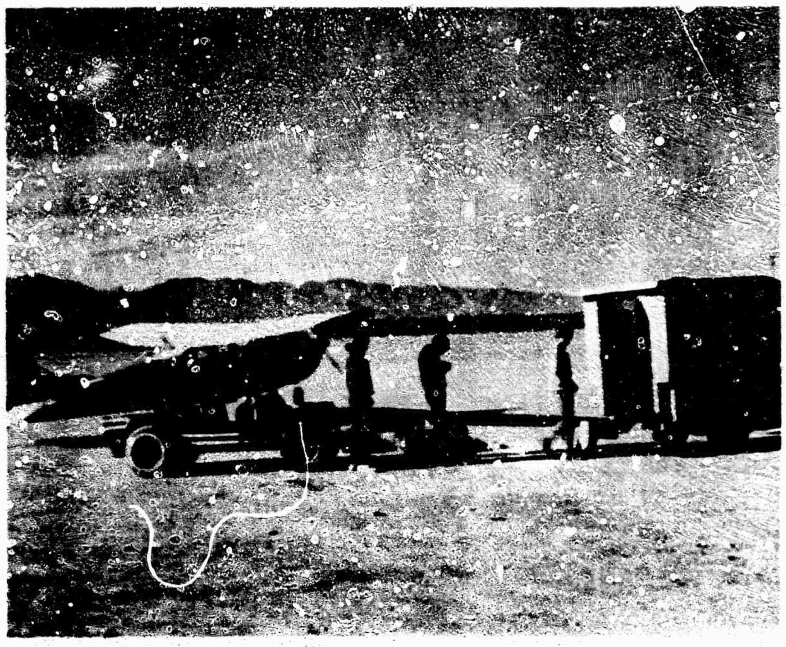

Fig. 9. FIELD EQUIPMENT ON LOCATION AT EL MIRAGE DRY LAKE

The measured wind at the flight level (determined by measurement of the speed at which the wake drifted) was generally from the west and perpendicular to the usual flight path. As Table 4 shows, the wind speed v ranged from calm up to 6.8 m/s (13 knots). The measured lapse rate γ at the flight level ranged from an extreme inversion (+16°C/100 m) during some low level tests near the ground to the slightly unstable level of -1.3°C/100 m, with the range at the normal altitudes being +1.6 to -1.3°C/100 m. The measured turbulence levels varied from negligible ($\epsilon^{1/3} \sim 0.2$ cm$^{2/3}$ s^{-1}) up to light-to-moderate ($\epsilon^{1/3} \sim 2.5$ cm$^{2/3}$ s^{-1}).

Both turbulence and lapse rate can influence the motion of the wake in many ways, some of which have already been discussed. There is, however, a correlation between atmospheric instability and turbulence, since an unstably stratified atmosphere is turbulent by definition (almost!). Turbulence created by shearing flow can be present even under stable stratification. with the effect of the stability being to suppress vertical spreading of the turbulent region. For these experiments, it was necessary to ascertain the degree of correlation between the turbulence level and the lapse rate in order to determine whether $\epsilon^{1/3}$ and γ could be treated as independent variables in a functional relationship of the form

$$\text{wake motion} = f(\gamma, \epsilon^{1/3}) .$$

Table 4

SUMMARY OF ATMOSPHERIC AND FLIGHT CONDITIONS

Date 1971	Pass	Time PST	h mAGL	T °C	$\epsilon^{1/3}$ $cm^{2/3}s^{-1}$	γ °C/100m	Wind m/s	V m/s	Hdg.
5/25	1	0513	107	18	2.2 v	+0.6	W 2.8	35	S
	2	0525	110	18	2.5 v	-1.0	W 5.3	35	S
	3	0543	134	18	0.8 v	-1.0	W -	32	S
	4	0553	140	19	2.0 v	-0.3	W -	35	S
	5	0610	232	19	0.7	-1.0	W -	32	S
8/31	1	0545	131	18	[illegible].4 v	0	W 6.8	32	S
	2	0551	131	18	1.4 v	0	W 3.5	32	S
	3	0619	143	17	2.4 v	+0.6	W 4.7	32	S
	4	0629	143	18	2.2 v	+0.8	W 5.3	32	S
	5	0650	158	17	2.0 v	-1.3	W 4.3	32	S
	6	0676	158	18	2.3 v	-1.0	W 6.4	32	S
	7	0717	143	18	2.0 v	-1.3	W 4.9	32	W
	8	0729	158	18	1.5 v	-0.7	W 6.8	32	W
11/3	1	0722	143	14	0.35	0	E 2.0	35	S
	2	0733	143	14	0.30	0	E 3.0	32	S
	3	0752	143	14	1.0 v	0	E 2.8	35	S
	4	0813	158	12	0.6 v	0	E 3.8	35	S
	5	0835	143	14	0.4 v	0	E 4.4	28	S
	6	0841	143	15	1.3 v	-0.3	E 2.9	58	S
	7	0857	10	11	2.0	+3.6	W -	30	S
	8	0905	131	14	2.0 v	-0.3	W 1.8	32	W
11/4	1	0620	143	14	0.30	+1.3	W 1.0	28	S
	2	0628	137	14	0.35	+1.3	W 1.4	29	S
	3	0644	143	14	0.30	+1.3	W 1.1	28	S
	4	0654	143	15	~0.6 v	+0.8	W 0.7	28	S
	5	0712	143	14	0.25	+1.3	W 1.6	28	S
	6	0723	149	14	0.35	+1.6	W 2.0	28	S
	7	0739	28	10	0.5 v	+1.6	W 0	29	S
	8	0743	8	7	1.5 v	+1.4	W 0	28	S

NOTES: h - height above ground level (AGL) at which pass was made and atmospheric conditions were measured.

$\epsilon^{1/3}$ - a value followed by v denotes variability of turbulence in time and space

γ - neutrally stable (adiabatic) lapse rate is -1.0°C/100 m.

Wind - wind speed is preceded by general wind direction (point of compass from which wind is blowing). A dash denotes that wind speed is unknown.

Hdg. - aircraft heading (point of compass toward which aircraft is headed).

Figure 10 is a plot of the turbulence and lapse rate dates of Table 4. As can be seen, any one value of stability corresponds to a wide range of turbulence levels, and vice versa. There is, however, a discernible trend in the expected manner, i.e., increased stability corresponds to decreased turbulence in general (if the three low altitude, shear dominated, points are ignored. If any conclusion can be drawn from this, it is that, for these experiments, the turbulence and lapse rate can be considered to be uncoupled to first order, but that sufficient coupling does exist to preclude any assumption of complete independence.

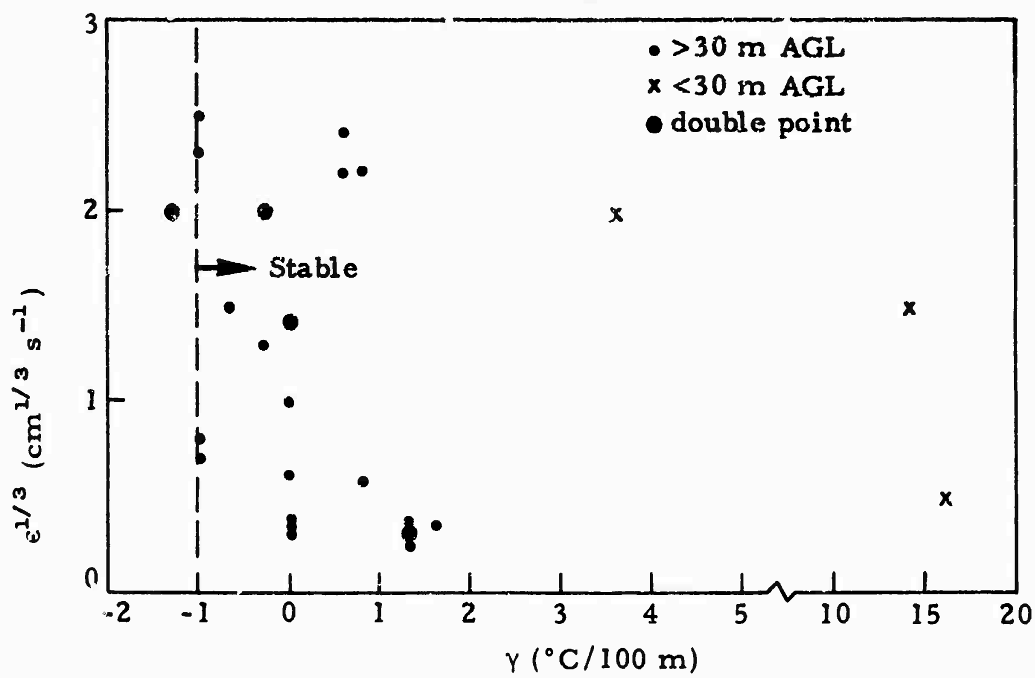

Fig. 10. PLOT OF TURBULENCE VS. LAPSE RATE FOR FLIGHT TESTS

3.2 Qualitative Observations of Wake

Since photography was the main technique used to observe the wake, a good deal of information was obtained by study of the films and still photographs of the vortices. In addition to a considerable amount of quantitative data which was obtained by measurements of the photographs, and which will be reported on in Section 3.3, there were many interesting phenomena which stood out to even a casual observer of the experiment or of a film of it. This section is devoted to a discussion of some of these "obvious" and also not-so-obvious phenomena.

Figure 11 is a view of the initial appearance of the smoke trails behind the Cessna 170. The red (left) vortex appears to be smaller in size and more sharply defined than the green (right) vortex. This was the cause of much puzzlement for quite a while, until it was found that the red smoke grenades used emitted smoke only from the bottom, while the green ones burned from both ends, resulting in a larger marked vortex on the green side. Some distance behind the aircraft, this "fuzzy layer" on the green vortex had diffused and both vortices were then of the same apparent size.

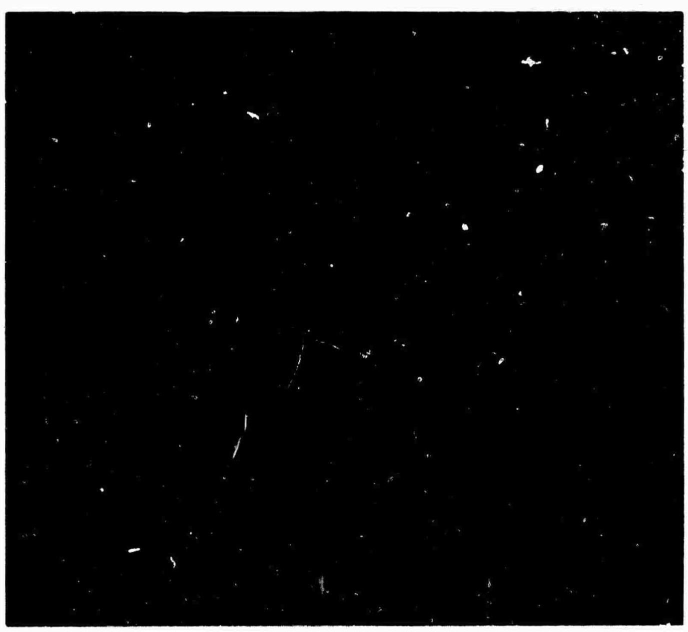

Fig. 11. INITIAL APPEARANCE OF SMOKE-MARKED VORTEX TRAIL (8-31, Pass 8)

Atmospheric motions were observed to influence the wake very shortly after aircraft passage, often as close as three spans behind it. The magnitude of this influence varied with the intensity of the atmospheric motions, with noticeable influence often taking some 20-30 seconds to manifest itself in very calm air, while a few seconds would suffice in turbulent conditions. Figure 12 shows this atmospheric influence over about 1/2 km of wake length (foreshortened considerably by a telephoto lens). In addition to small scale wiggles of the same scale as the diameter of the smoke trail, many segments of the wake have been influenced by atmospheric eddies whose scale is larger than the vortex separation. This particular wake was photographed in a near-neutrally stratified atmosphere ($\gamma = -1.3°C/100$ m) with light turbulence ($\epsilon^{1/3} \sim 2.0$ cm$^{2/3}$ s^{-1}), and it was destroyed by the sinuous instability about 18 seconds after generation.

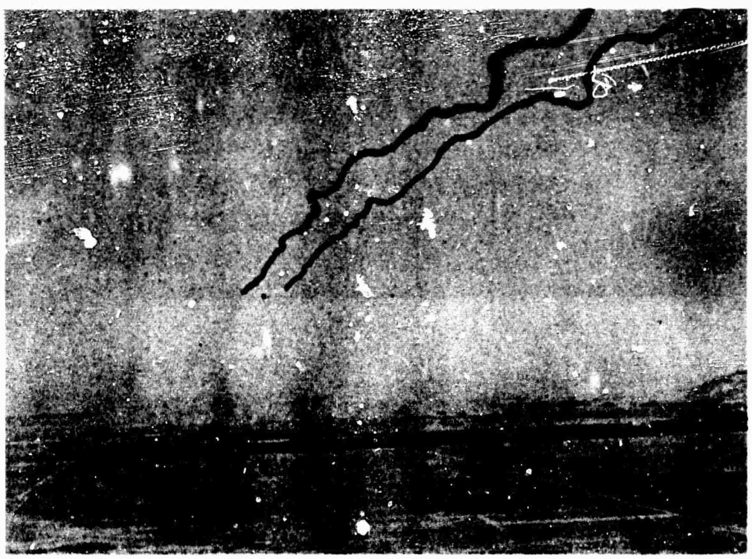

Fig. 12. EFFECT OF TURBULENCE ON WAKE (8-31, Pass 7)

In a very calm, stable atmosphere, the wake behaved very much in a textbook manner. As the sequence in Fig. 13 shows, the wake descended with only slight waviness and a small amount of vertical separation of the two vortices apparent after one minute. There was some slowing down of the descent speed, from 0.62 m/s at t = 0 (the theoretical value) to 0.31 m/s at t = 60 seconds. This particular wake had a lifetime of 65 seconds and was destroyed by a burst-type instability (which will be discussed below).

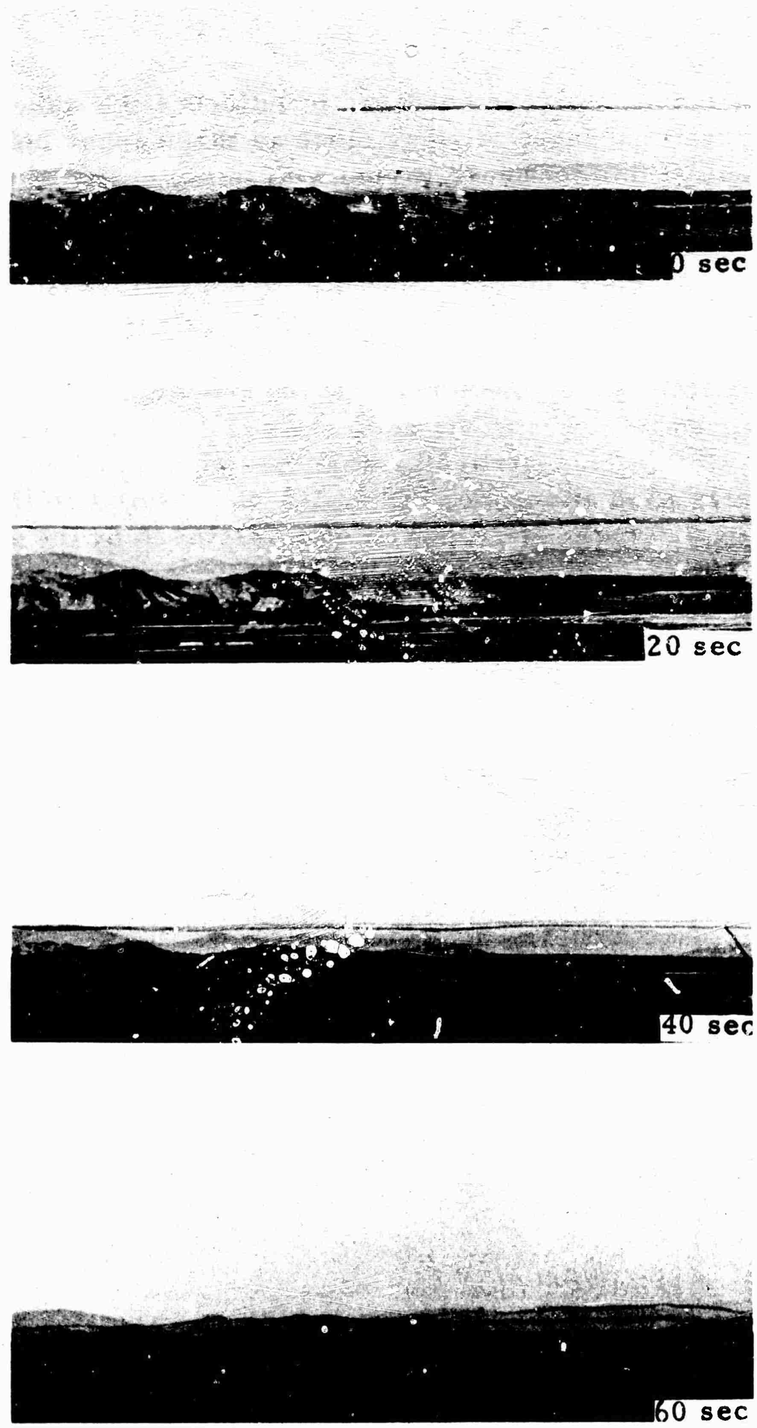

Fig. 13. SIDE VIEW OF WAKE IN CALM, STABLE ATMOSPHERE AT 20-SECOND INTERVALS (11-4, Pass 1)

The vortex system rarely behaved in this manner, however. One disturbing characteristic was the tendency of the vortex system to roll onto its side, as the sequence in Fig. 14 shows. This occurred frequently, at all levels of stability and turbulence, although the degree of roll varied. Figure 13 showed a relatively small amount while Fig. 14 shows an extreme case where the wake has rolled past the vertical and the average vortex spacing at t = 80 seconds is 1.2 times the span, or about 1.5 times the normal spacing. Burnham, et al., (1972) have observed a similar rolling tendency for jet transport wakes near the ground.

No satisfactory explanation has been found for this rolling tendency. Since the aircraft was usually only some 130 m above the surface it was still in the atmospheric boundary layer and hence any wind, which was usually perpendicular to the flight path, was actually a vertically stratified shear flow. Consideration of vortex kinematics in such a flow could explain the often observed tendency of the upwind vortex to become the lower vortex. There were several cases, however, where the downwind vortex was the one which descended, which cannot be as easily explained. Data for Burnham, et al., show a similar pattern with the upwind vortex usually, but not always, descending lower than the downwind one.

The last photograph in Fig. 14 shows an often-observed mode of catastrophic decay of the vortices, which was seen over the entire range of atmospheric and flight conditions encountered in this test series. This type of decay manifests itself as a localized "burst," or sudden increase in diameter, of a single vortex core, followed by travel of a conical parcel of smoke down the vortex. Figure 15 is a sketch of the apparent appearance of this region as ring vortices encircling the core which travel along the vortex. There is usually little or no smoke left behind this traveling region, while the density of smoke within it increases as it moves down the core. This suggests that at least some of the smoke initially in the core is swept up into these rings.

Figure 16 is a photograph of a vortex core being destroyed by two of these instabilities. The two bursts, which were traveling toward each other, collided a few seconds later at the center of the picture, leaving behind an intensely marked disc-like parcel of smoke. The normal burst travels along the core toward the generating aircraft, but frequently (particularly in older vortices) bursts were seen to travel away from the aircraft, or a burst would result in two of the conical regions traveling away from each other and leaving a smoke-free volume in between.

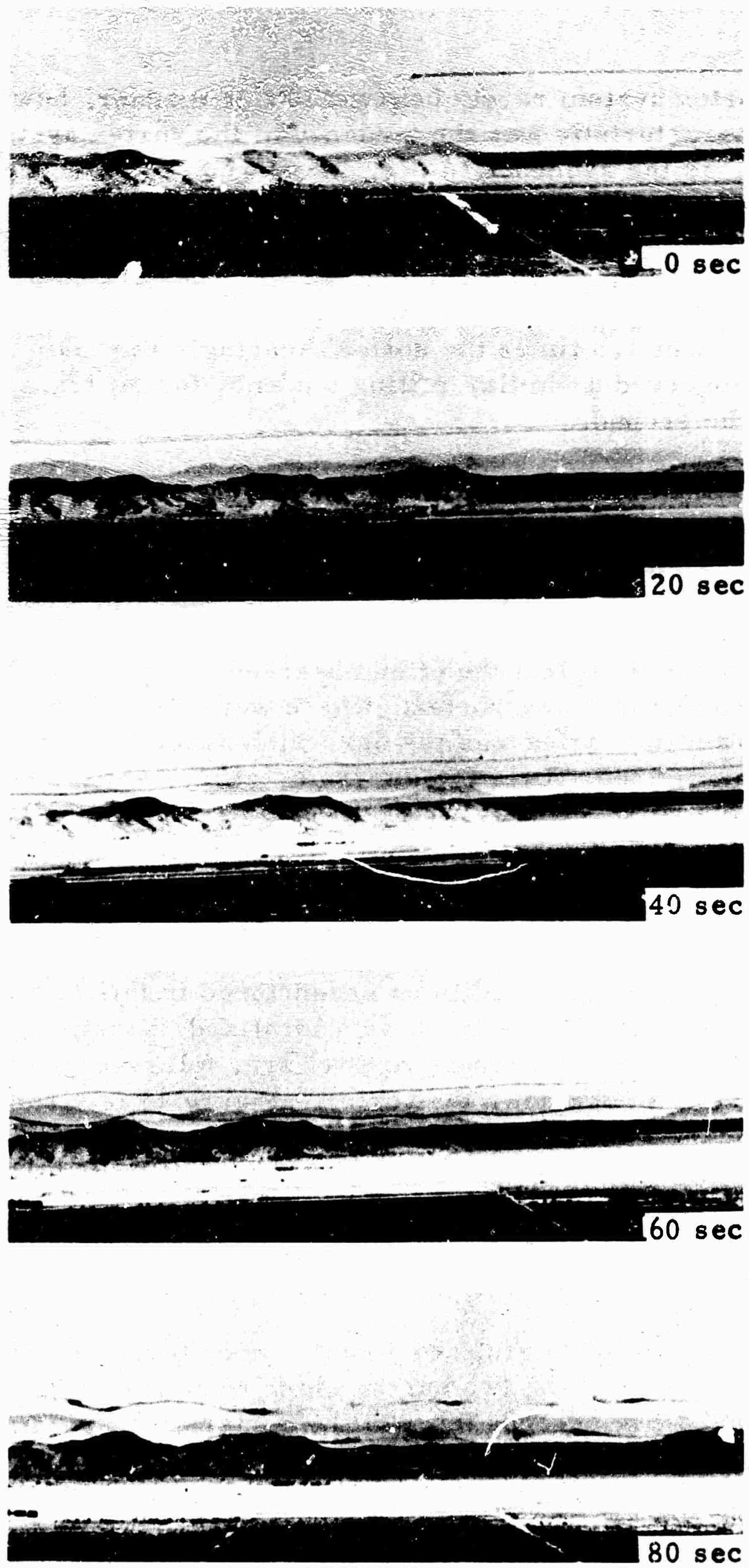

Fig. 14. SIDE VIEW OF WAKE IN CALM, STABLE ATMOSPHERE AT 20-SECOND INTERVALS, SHOWING ROLLING TENDENCY AND DESTRUCTION BY CORE-BURST INSTABILITY

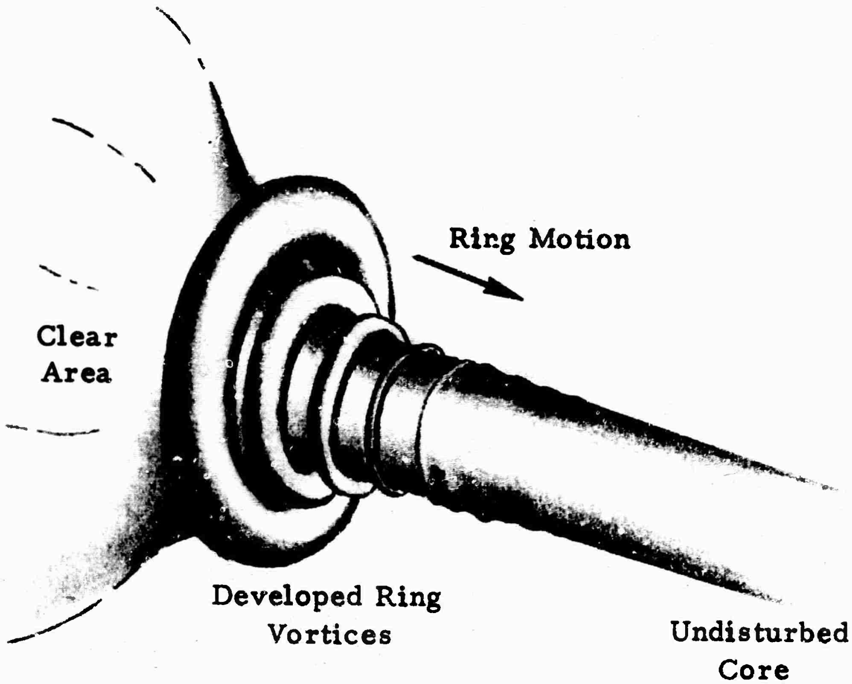

Fig. 15. SCHEMATIC REPRESENTATION OF POSSIBLE CORE BURST CONFIGURATION

Fig. 16. DETAIL OF CORE DESTRUCTION BY BURSTING

Bursting of trailing vortex cores has been observed before, particularly in small scale water tank tests (Widnall, Bliss, and Zalay, 1971; Olsen, 1971) where it appears to be the dominant mode of vortex decay. Full scale flight tests may also display the same form of instability (FAA Task Force, 1971) and it has been observed in wind tunnel experiments (Hackett and Theisen, 1971). A similar type of instability can be seen in Fig. 2 of this report.

The cause of the burst and the details of it have not been completely understood. Olsen deduces that axial flow in the core plays a role. Hackett and Theisen found an adverse pressure gradient in a wind tunnel diffuser to be a contributory factor. In water tank tests, both they and Widnall, et al., found that the bursting could precede or follow the sinuous type vortex interaction. Harvey and Fackrell (1970) postulate that the bursting is a core-edge phenomenon related to a kinematic instability of elements of the vortex core, and show flow visualization experiments to support their tentative model. The appearance of the instabilities they saw was very much like those observed in the present experiment, except that their water tank photographs contain much greater detail and show clearly the formation of the ring vortices around the core.

The current experiments showed the core bursting to be independent of the sinuous instability, since bursting was observed at all points along the vortex and it did not seem to have any relation to the curvature of the vortex filaments or to their local separation. This is at variance with the observations of Widnall, et al., who state that the bursts were observed in the "high pressure regions where the vortices are farthest apart" and are coupled with the sinuous instability, and Scorer (1958) and Scorer and Davenport (1970) who describe "bursts" at the point of least separation of the vortices.

As was stated above, the core bursting instability was observed at all levels of turbulence and atmospheric stability. The sinuous (Crow) vortex interaction was also observed in these experiments, but rarely at low levels of turbulence. Figure 17 shows the breakup of a vortex trail by both bursting and mutual interaction and linking in light turbulence and neutral stability. Figure 18 is a detail view of a portion of the same sequence, taken with the 16-mm camera at Site 2. It can be seen that the linking is preceded by a rapid downward acceleration of those portions of the vortex trail which are closest together, and the actual contact takes place in a near-vertical plane.

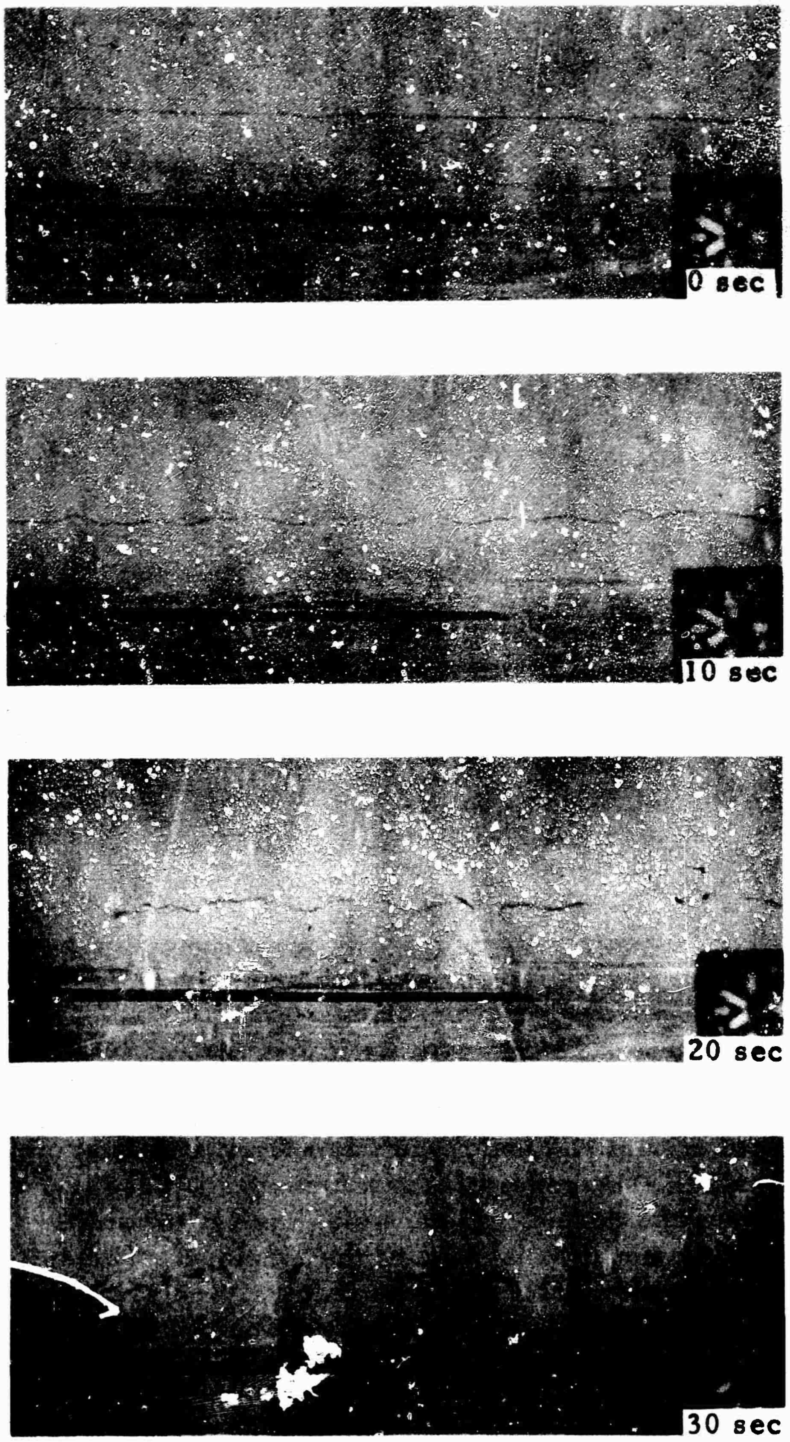

Fig. 17. SIDE VIEW OF WAKE AT 10-SECOND INTERVALS, SHOWING DECAY BY LOCALIZED VORTEX BURSTING AND BY INTERACTION OF VORTICES. Note the saddle shaped vortex ring at t = 30 sec (8-31, Pass 5).

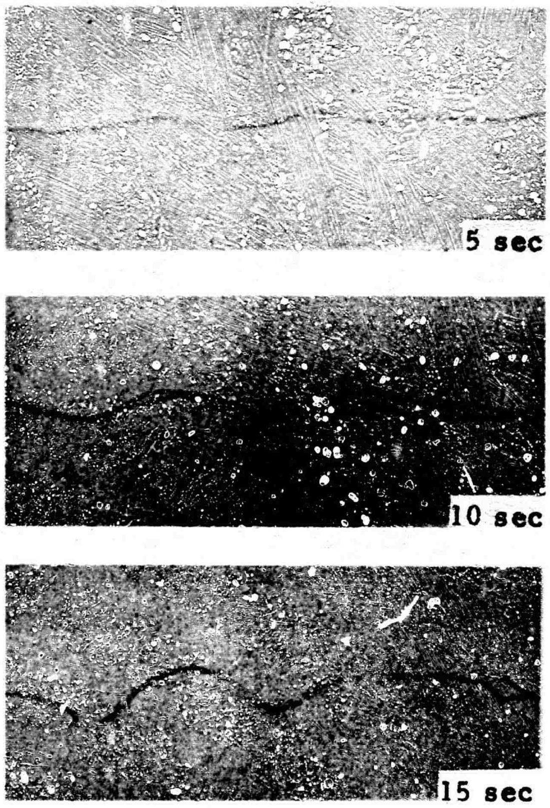

Fig. 18. DETAIL SIDE VIEW OF GROWTH OF SINUOUS INSTABILITY AND LINKING OF VORTICES (8-31, Pass 5)

Figure 19 shows the development of the sinuous instability, as seen from below the wake. This particular sequence, which is exceptional for its clarity and detail, is taken from a motion picture made in 1963 by MRI. The generating airplane was a Cessna 180, grenade smoke marked the cores, and the white haze is oil smoke from oil injected into the hot exhaust pipe of the airplane. The spiral wavelets on one linked portion are a common feature, and are also visible in Fig. 2. The three-dimensional nature of the linking, resulting in saddle-shaped vortex rings, can be visualized from the preceding three figures. The similarity of the sequence in Fig. 19 to the water tank series photographed by Hackett and Theisen (1971) is striking.

Figures 20 and 21 are two general interest views of the wake. Figure 20 is a complicated scene showing a point where the vortices have linked into loops and where the right loop has subsequently burst with the conical smoke regions moving off to the right of the picture. The left

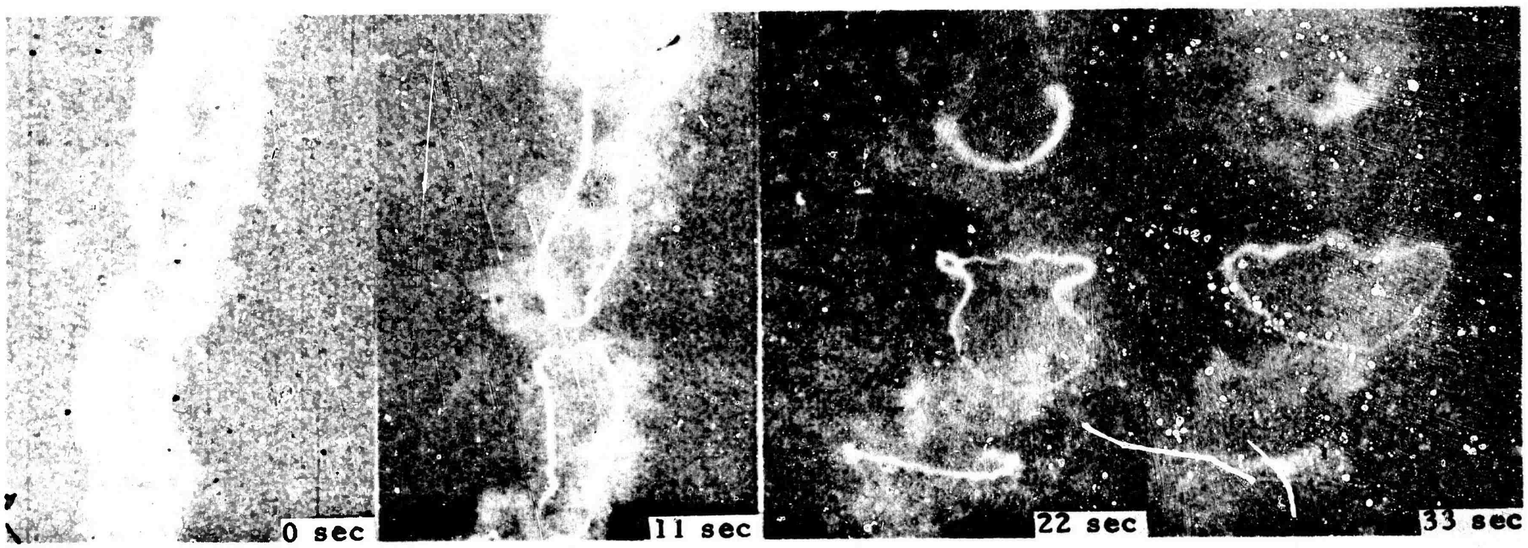

Fig. 19. EVOLUTION OF SINUOUS INSTABILITY, AS SEEN FROM BELOW, AT 11-SECOND INTERVALS

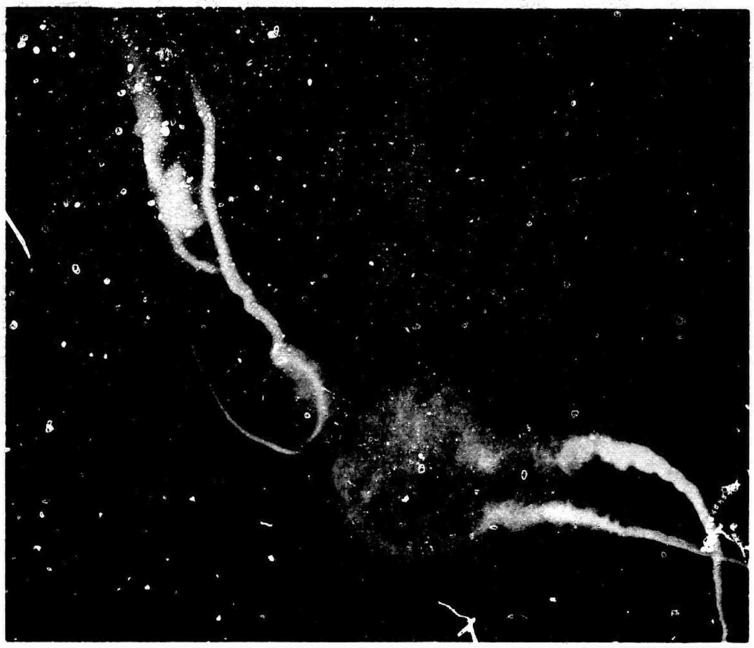

Fig. 20. SIMULTANEOUS OCCURRENCE OF VARIOUS FORMS OF INSTABILITY. This photograph was taken from below and slightly to the side of the wake (11-4, Pass 6)

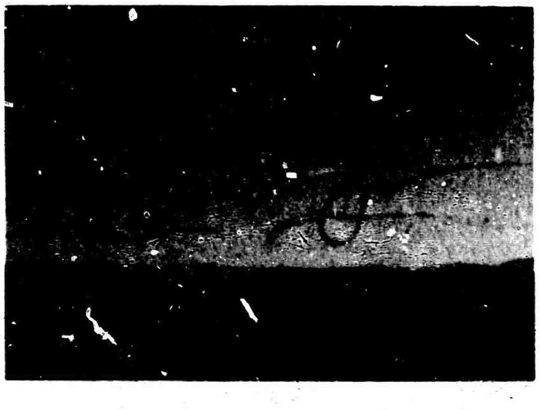

Fig. 21. CLOSEUP VIEW OF LINKED VORTICES, PHOTOGRAPHED FROM THE AIRPLANE FLYING THROUGH ITS OWN WAKE Another wake is in the background.

loop is well defined at the point of joining, but is convoluted and bursting at the edge of the photograph. An aerial closeup of a linked vortex appears in Fig. 21. This photograph shows the very clean nature of the linking, with no smoke residue left outside the cores at the point of contact, and the near-vertical orientation of the loop is apparent. For this picture, the airplane flew several consecutive passes, making wakes and photographing them; some results of earlier passes are visible in the background.

3.3 Measurements of Wake Motion and Decay

Certain aspects of the wake motion can be discerned in a quantifiable manner from photographs of the smoke-marked trail. In the current program, the lifetime of the wake was measured and the descent and separation of the vortices were determined as functions of time.

The easiest measurement to make was that of the age of the wake at the time when a burst or sinuous type instability appeared. Figure 22 shows the time at which the first instability appeared on any given pass, plotted as a function of turbulence. This time was defined by the point at which a burst had progressed sufficiently far to leave a small clear space in the smoke trail or when the two vortices had actually made contact. Several interesting features are apparent. First, the few linking points fall on the same general wave as the burst points. Second, there is a general $1/\epsilon^{1/3}$ behavior of the data, with a reasonable expression defining the time before which an instability will usually not occur being

$$t_1 = \frac{15}{\epsilon^{1/3}} \text{ sec}$$

for ϵ in cgs units. This curve is plotted on the figur Third, the general effect of atmospheric stratification is weak, t there is an apparent tendency toward increased wake lifetime as the stability increases while the turbulence remains constant.

Also of interest is the total lifetime of the wake. Figure 2: is a plot of the time at which the wake on each pass was completely destroyed by instability, so that there was no longer any organized motion apparent. The points here represent the final instability observed — the coup de grace for the wake. Again a $1/\epsilon^{1/3}$ behavior is apparent, with the upper bound (the time at which the wake is usually destroyed) represented fairly well by

$$t_2 = \frac{70}{\epsilon^{1/3}} \text{ sec,}$$

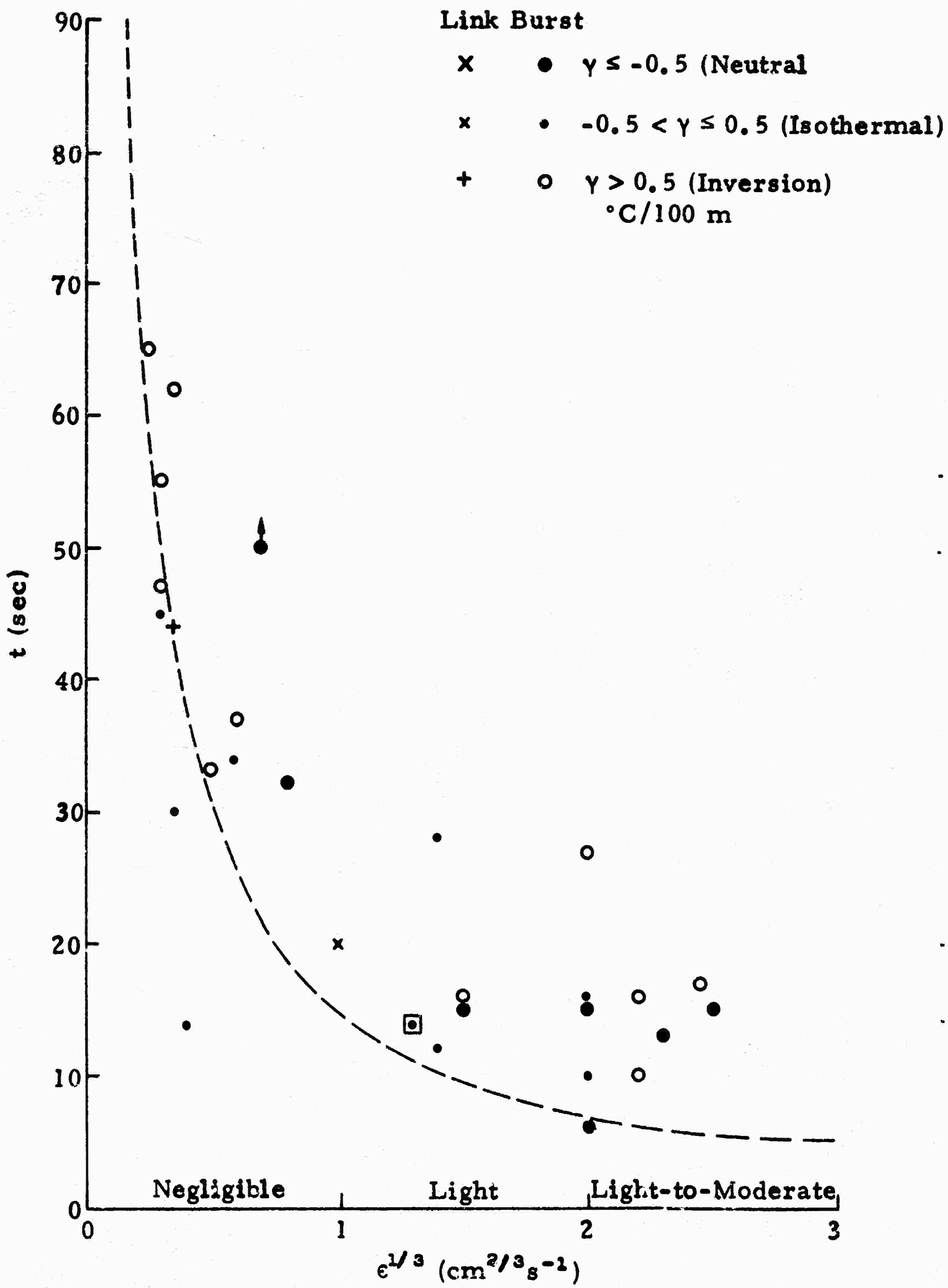

Fig. 22. PLOT OF TIME OF FIRST OBSERVED INSTABILITY AS A FUNCTION OF THE TURBULENCE LEVEL $\epsilon^{1/3}$
All points had $\Gamma \sim 30\ m^2/s$ except for the one point marked ▣, where $\Gamma = 16\ m^2/s$. An early bound to the data is shown. The point with an arrow indicates that an instability had not appeared at the indicated time but that data for a longer time is not available.

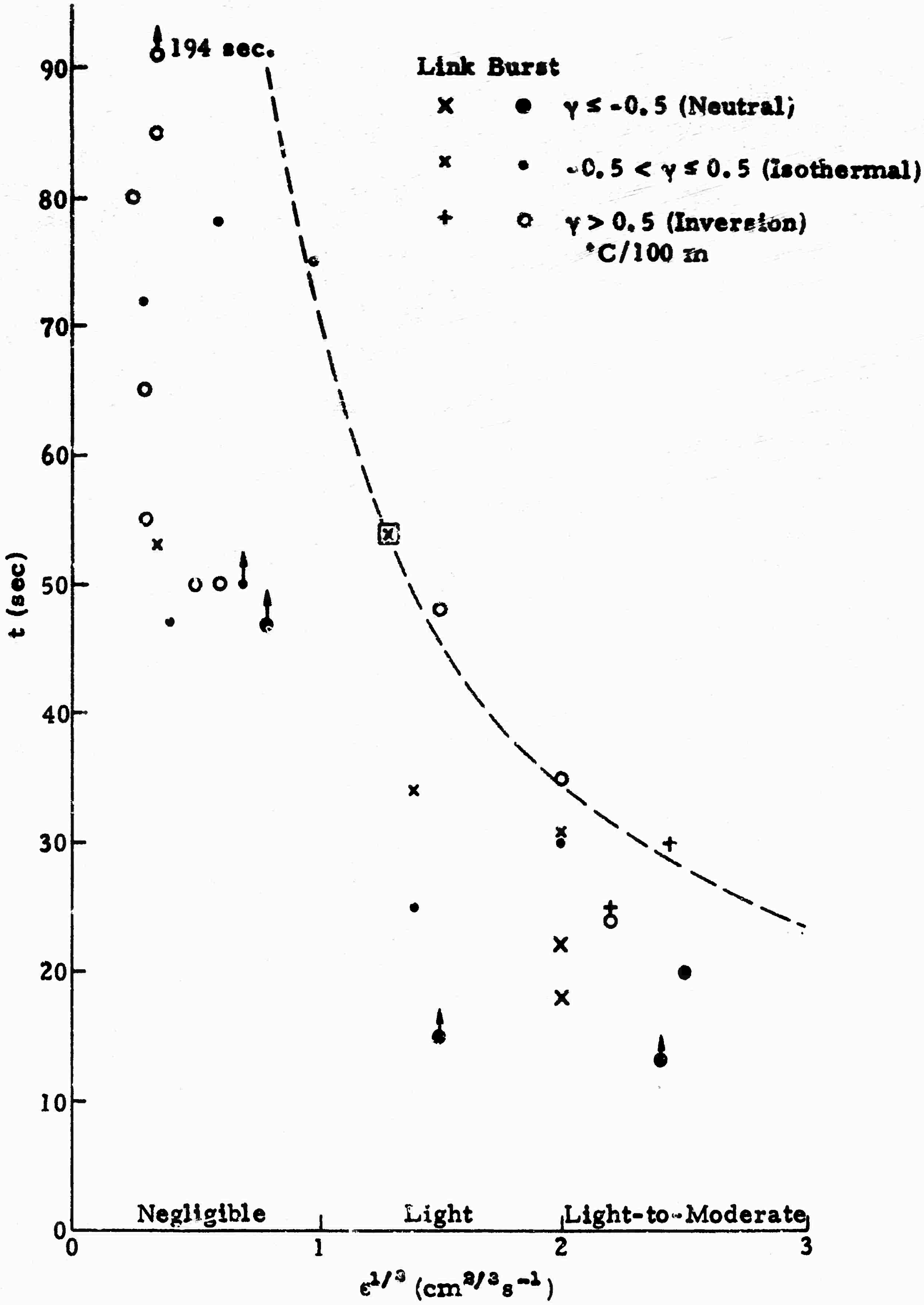

Fig. 23. PLOT OF TIME OF DESTRUCTION OF WAKE AS A FUNCTION OF THE TURBULENCE LEVEL. An upper bound curve is indicated. The points with arrows denote that the wake was still present in some organized manner at that point, but that further data is not available.

although the scatter is considerable. This curve is plotted on the figure. The same comments about atmospheric stability and the natures of the types of instabilities apply here as for Fig. 22.

The one point at $t = 194$ sec is a somewhat unusual one which carries disturbing implications for the prediction of jet transport wake lifetimes. In this case, one vortex was destroyed by a bursting instability at an age of 65 seconds. Its mate thereupon remained fixed in space (except for drift with the wind) with no apparent change in vortex structure for at least two more minutes. The camera filming this event ran out of film at $t = 194$ sec, so the ultimate fate of this vortex is unknown. A similar case where a single B-52 vortex persisted for some 6-7 minutes has been reported by MacCready (1971) and Burnham, et al., (1972) mention one Boeing 747 vortex which persisted near the ground for at least three minutes. In all of these cases, the common feature was the destruction of one vortex, which thereby precluded the appearance of a sinuous type instability. Whatever mechanism suppressed the bursting of the remaining vortex is not known.

Figure 24 is a plot, on a logarithmic grid, of all instabilities observed during the 29 test flights, which gives a feel for the time span over which the breakup of the wake was taking place. The two envelope equations suggested above are plotted here also for reference.

Figures 22-24 show one data point set (marked with small boxes) where the circulation ($\Gamma = 16\ m^2/s$) was about half that for the other points (where $\Gamma \sim 30\ m^2/s$). Although the data scatter is too great to permit a definite conclusion, it appears that there is no strong effect of circulation on the life of the wake. Crow (1970) predicts that the amplification time constant for the sinuous instability should vary as Γ^{-1}, with the computed value from his formulas being 19 sec for $\Gamma \sim 30\ m^2/s$ and 35 sec for $\Gamma = 16\ m^2/s$. The data shows several vortex linkings which have taken place at wake ages of from one to two of these time constants, which is much faster than Crow's observation (using the photographs reproduced in Fig. 1 of this report) that linking requires about three time constants. There is a correlation between time-to-linking and turbulence level, as has already been noted, and at low turbulence levels the observed points do approach an age of about three amplification time constants. This suggests that the purely kinematical instability treatment by Crow gives a lower bound to the rate of amplification of the sinuous instability, and that turbulence is able, through some yet undefined mechanism, to increase the speed at which the instability grows.

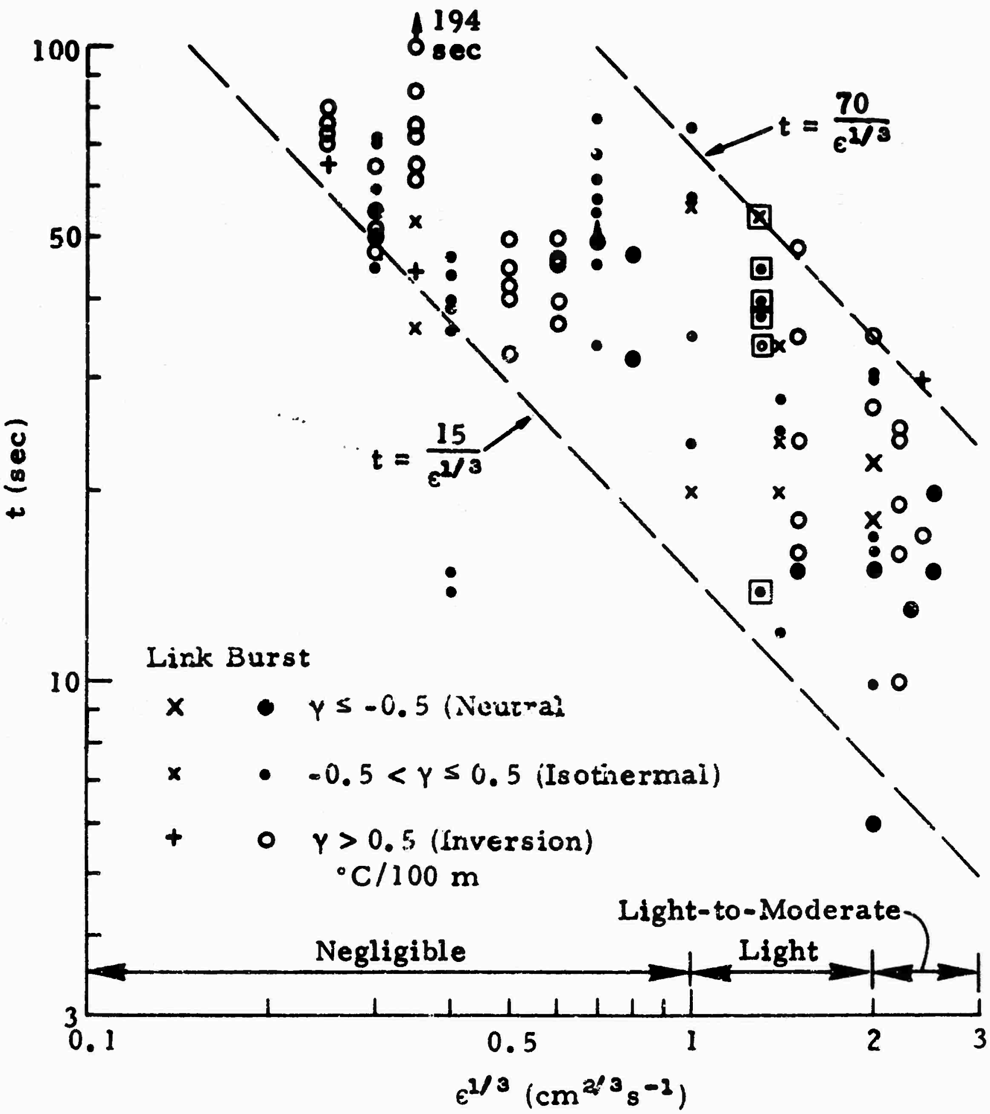

Fig. 24. TIME OF OCCURRENCE OBSERVED INSTABILITIES AS A FUNCTION OF TURBULENCE

Figure 25 shows the same date as in Fig. 24, but plotted against the lapse rate. The strong effect of atmospheric stability on increasing the life of the wake is quite apparent, but the coupling between turbulence and stability which was demonstrated in Fig. 10 (and which shows here since the dark points corresponding to low turbulence tend to appear at greater stabilities than the lighter points for greater turbulence) must be recalled. The clusters of points in the right half of the graph correspond to wakes which were generated in ground effect, or which descended into ground effect, and their independent behavior from the remaining data suggests that atmospheric stability is not a major factor controlling wake lifetime. The few $\Gamma_0 = 16\ m^2/s$ points on Fig. 25 appear to fall in with all the others for $\Gamma_0 \sim 30\ m^2/s$, **hence there appears** to be no stability and circulation interaction governing wake life.

The descent of the wake was measured from the Site 2 films. To eliminate the effects of localized perturbations on the determination, several measurement points were chosen along the approximately 1/2 km wake length visible in the photographs and the measurements from these points were averaged. Some trajectories thus obtained are plotted in Figs. 26 and 27. No effort was made at further analysis of the data because the strongest influence on the wake descent appeared to be the variable tendency of the wake to roll over and thereby change the downward component of the velocity induced by each vortex on the other. The values for Δh on the figures indicate the largest average vertical separation of the vortices (+ means red below green, - means green below red) where it should be noted that the vortex spacing for a horizontal vortex pair is 8.7 m. There is no apparent effect of atmospheric stability on the descent, but it may have been masked by the rolling tendency.

With one exception, all of the wakes descended initially at a speed very nearly the theoretical value,

$$w_0 = \frac{\Gamma_0}{2\pi b},$$

if the vortex spacing is taken to be the elliptical lift distribution value of $\pi/4 \times$ span (or 8.7 m). (This descent rate is marked on the figures.) After some time, a slowing down of descent was observed and, in some cases, the wake leveled off or even rose upward. Although this pattern of motion is quite reminiscent of that shown in Fig. 4, the complication resulting from a non-horizontal vortex plane makes it difficult to read much into this resemblance.

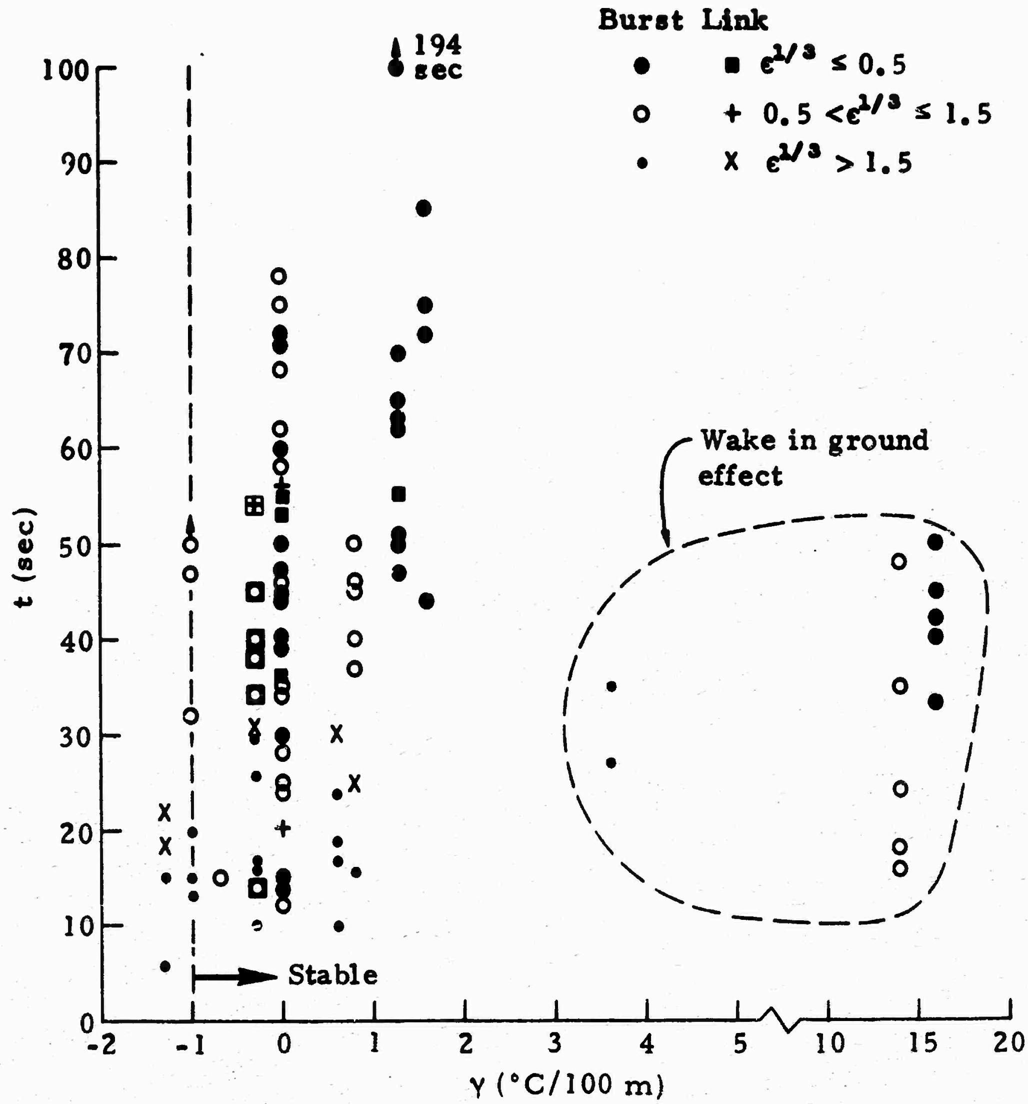

Fig. 25. TIME OF OCCURRENCE OF WAKE INSTABILITIES AS A FUNCTION OF ATMOSPHERIC STRATIFICATION
$\Gamma_0 = 16\ m^2/s$ for the boxed points; otherwise $\Gamma_0 \sim 30\ m^2/s$.

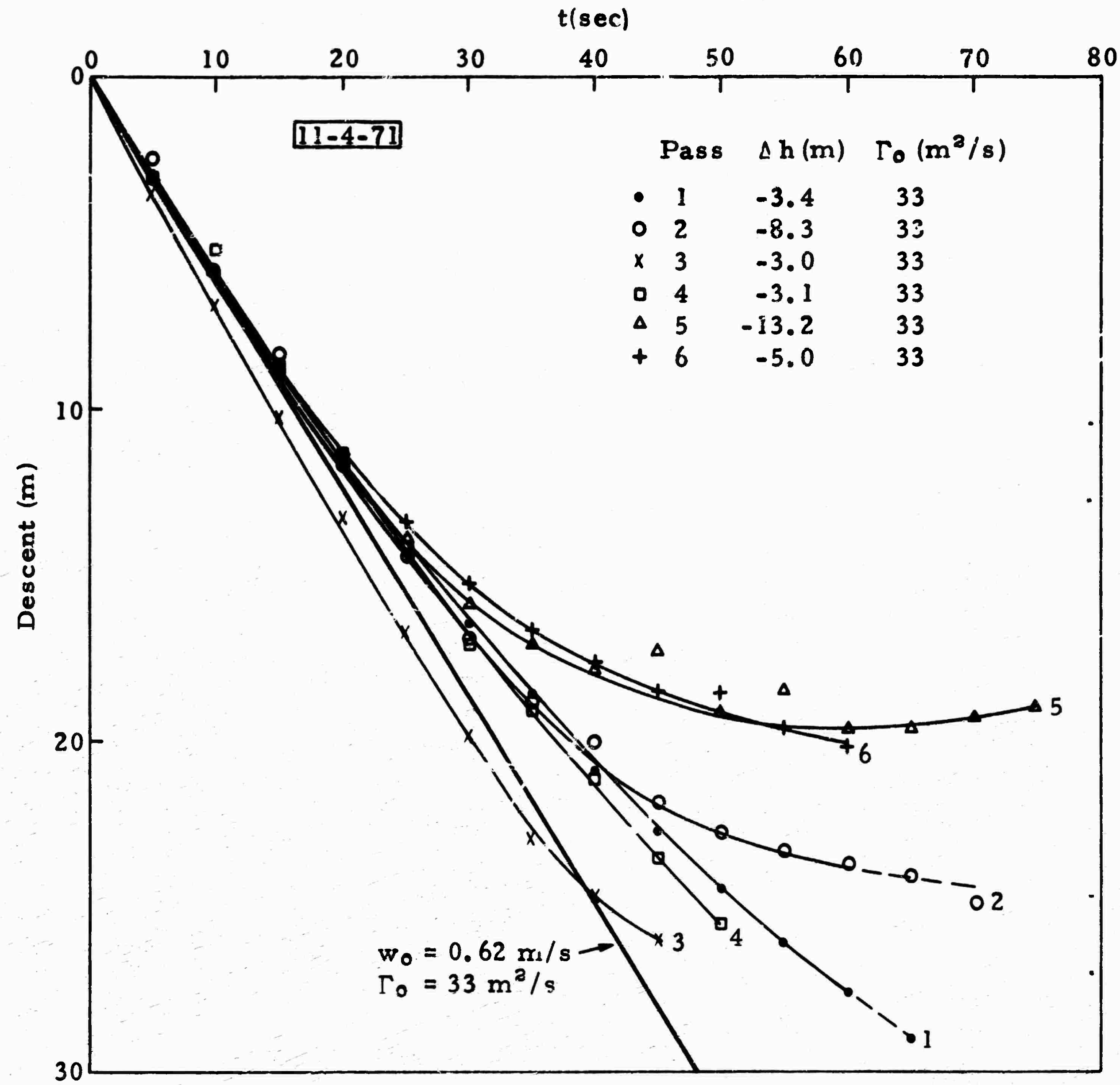

Fig. 26. TRAJECTORIES OF WAKE DESCENT IN A STABLY STRATIFIED ATMOSPHERE ($\gamma \sim 1\,°C/100$ m, AN INVERSION) WITH NEGLIGIBLE TURBULENCE ($\epsilon^{1/3} \sim 0.3\ cm^{2/3}s^{-1}$)
Δh is the maximum observed vertical vortex separation. The theoretical initial descent rate is shown. Broken lines indicate less reliable data. (11-4, Passes 1-6)

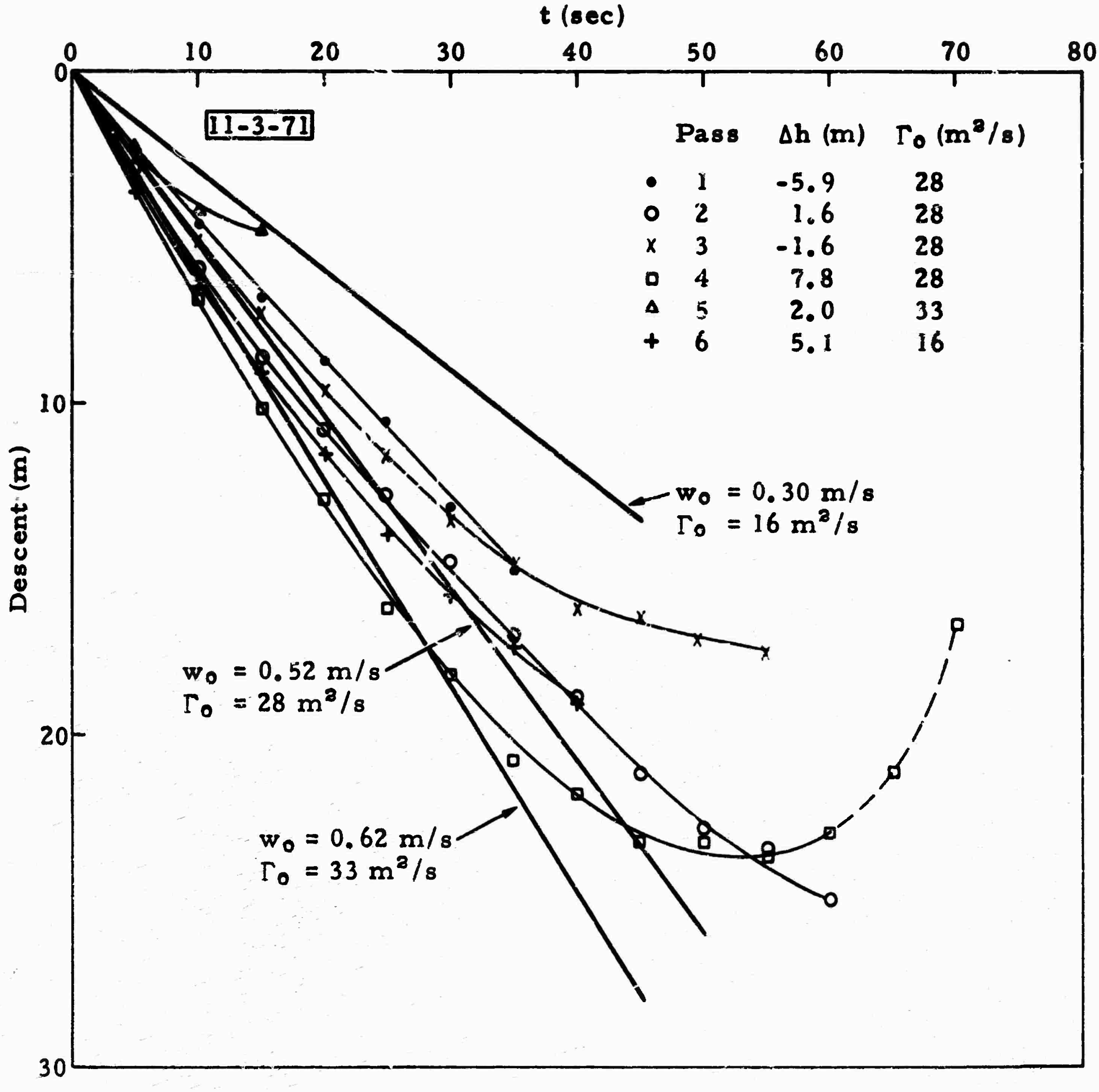

Fig. 27. TRAJECTORIES OF WAKE DESCENT IN AN ISOTHERMAL, STABLY STRATIFIED ($\gamma \sim 0°C/100$ m) ATMOSPHERE WITH NEGLIGIBLE TURBULENCE ($\epsilon^{1/3} \sim 0.35$ $cm^{2/3}s^{-1}$ FOR PASSES 1-2, 4-5) OR LIGHT TURBULENCE ($\epsilon^{1/3} \sim 1.1$ $cm^{2/3}s^{-1}$ FOR PASSES 3 AND 6)
Δh is the maximum observed vertical separation. The theoretical initial descent rates for all cases are shown. Broken lines indicate less reliable data. (11-3, Passes 1-6)

The one wake which did not behave as expected is the one for Pass 6 on Fig. 27, where the circulation should have been half of that of the other passes and thus w_0 should have been halved. For reasons unexplained, this speed was about the same as for the other passes. The sudden leveling off and breakup of Pass 5 on 11-3 is also puzzling.

A few wakes were generated near the ground. Their descent is plotted on Fig. 28. In all cases, the atmospheric stability was strong (a strong inversion) while various levels of turbulence were encountered. The one wake generated out of ground effect (11-4, Pass 7) behaved much the same as the ones discussed previously, except that its descent was slowed more preceptibly at an earlier time. One pass at wingspan height (11-3, Pass 7) resulted in a wake which appeared to be leveling off near the expected height of $b_0/2$. The final pass was made at a very low altitude (11-3, Pass 8) and its wake appeared to level off at about 2 meters above the ground, although difficulties in taking measurements from the film at this low elevation result in a fair amount of data scatter and uncertainty.

Finally, some attempts were made to measure the vortex spacing for correlation with the various theoretical predictions of Section 2, but since the wake had a tendency to roll, these measurements were difficult to make and their utility for the desired correlation was questionable. Suffice it to say that, for essentially level wakes, the vortex spacing was initially very nearly 0.8 times the wingspan and it tended not to vary too greatly from that value as the wake descended. The usable data is fairly meager, but if any change in vortex spacing with descent could be detected, it appeared to be a slight increase to up to 1.2 b_0 (or about one span). As was noted earlier, though, vortex separations in excess of a wingspan were observed in wakes which had rolled completely onto their sides.

	Date	Pass	γ(°C/100 m)	$\epsilon^{1/3}$ ($cm^{2/3}s^{-1}$)	Δh (m)
o	11-3	7	+3.6	2.0	-1.4
•	11-4	7	+16	0.5	2.7
×	11-4	8	+14	1.5	0.6

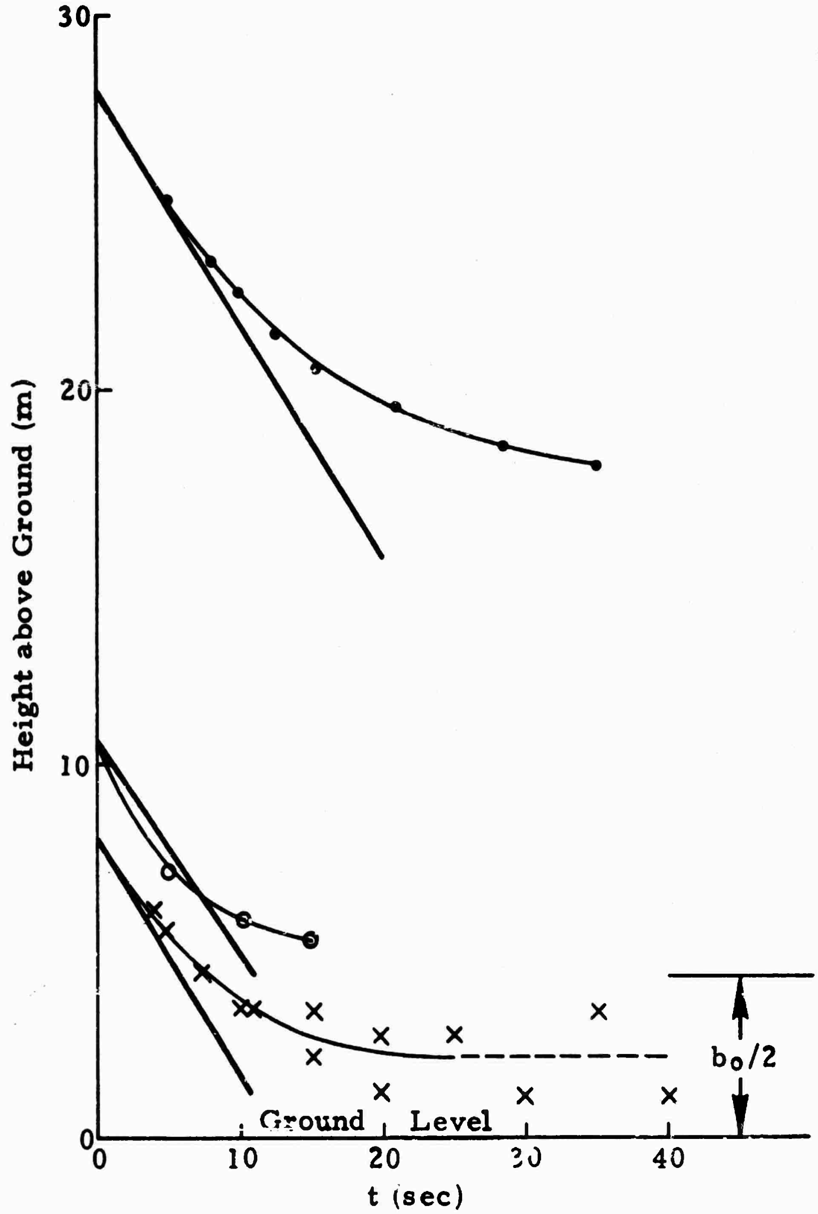

Fig. 28. WAKE TRAJECTORIES NEAR THE GROUND
$\Gamma_0 \sim 30\ m^2/s$ for all cases. The predicted initial descent speeds are shown, as is the theoretical leveling-off point.

4. CONCLUSIONS

This report has contained discussions of a variety of theoretical and experimental points about wakes, including not only observations made under the AFOSR-sponsored study, but also simultaneous work by others. It might be useful to summarize briefly some of the salient points.

First, the experimental study yielded the following observations:

1. The vortices were never observed to decay due to viscous or turbulent dissipation, but were always destroyed by some form of instability.

2. Two modes of instability were observed. One was a localized "bursting" of the smoke-marked core of an individual vortex, usually with no apparent effect on the adjacent vortex or on distant segments of the same vortex. The other instability was the well-known sinuous instability of both vortices which results in their linking into vortex rings. The linking was observed to be a very "clean" process, with no visible smoke residue left behind. In these experiments, the bursting was the dominant mode of decay.

3. There is a clear correlation between wake lifetime and atmospheric turbulence. The life of the wake is dramatically shortened by even small amounts of turbulence. Interestingly, for these particular tests, the lifetime at any particular level of turbulence tended to be the same, regardless of whether decay was due to bursting or linking.

4. As has been observed before, if one vortex is destroyed by bursting, the other vortex will sometimes last a very long time. One such case was observed where the core of one vortex was still clearly defined by smoke at an age of 194 seconds.

5. There is also an apparent correlation of wake lifetime with the lapse rate but the effect is weak (if the turbulence level is fixed).

6. The majority of the wakes were observed to roll to some degree. A few rolled so much that the plane of the vortices was vertical or past the vertical.

7. Wakes out of ground effect usually descended between 1 and 2-1/2 spans before they were destroyed by an instability. In all cases,

the descent speed slowed as the wake descended, and a few wakes were observed to level off or even to rise upward. There was no observable correlation between wake descent and atmospheric stability because the motion appeared to be dominated by the variable rolling tendency of the wake.

8. The vortex spacing remained essentially unchanged during the descent of the wake, with a small increase in spacing being conceivable. Rolled wakes often had larger vortex separations.

The implications of the above for interpretation of the theoretical models discussed in Section 2 are not wholly clear. It is likely that all real wakes do level off if they live long enough, although the downward accelerating motion predicted by some models cannot be wholly dismissed. It also appears that the vortex spacing changes very slowly as the wake descends, and if it does change it probably increases. Until a better understanding of the mixing process between the wake and the atmosphere is acquired, it is unlikely that much further progress can be made theoretically, since quite different forms of behavior can be created by very small changes in entrainment models. The work by Tulin and Shwartz (1971) stands out as an excellent marriage of theory and experiment, but the method of vortex generation and the scale of the experiment were sufficiently different than those in aircraft operations so that utilization of their results without further study is not warranted.

The question of scale is also of relevance to the experiment series with the Cessna 170. The relationship between energy in the wake and that in the atmosphere should have some effect on determining the degree of atmospheric dominance of the wake motion. Wake instabilities are surely scale-dependent. In fact, it appears that the common mode of decay in very small-scale (or low Reynolds Number) experiments is the core bursting mode, while for experiments with large transport aircraft, it appears to be the linking mode. The separation is not quite clear-cut, though, and both modes have been observed at all scales. The coexistence of both modes in this experimental series, at essentially the same wake ages, is of interest, as is the fact that the incidence of both forms of instability is coupled to the turbulence level. What is not known, however, is how to apply this information to the wakes generated by large aircraft.

Finally, there is the annoying (for a theoretician) tendency for the wake to roll. This recently observed phenomenon, as well as the occasionally long-lived, single vortex phenomenon, both deserve further study since they would dominate wake behavior in operational situations. Clearly, the trailing vortex wake has not yet given up all her secrets. The author expects to probe deeper for a few more in the future.

5. REFERENCES

Bisgood, P. L., R. L. Maltby, and F. W. Dee, 1971: Some work at the RAE on the behaviour of vortex wakes. In Aircraft Wake Turbulence and its Detection (Ed. J. H. Olsen, et al.) Plenum Press, 171-206. Also RAE Tech. Memo AERO 1244.

Burnham, D., J. Hallock, R. Kodis, and T. Sullivan, 1972: Vortex sensing tests at NAFEC. Dept. of Transportation, FAA, Report No. DOT-TSC-FAA-72-2.

Crow, S. C., 1970: Stability theory for a pair of trailing vortices. AIAA J., 8, 2172-2179.

FAA Task Force, 1971: Vortex wake turbulence flight tests conducted during 1970. FAA Report No. FAA-FS-71-1.

Gannon, M. T., A. L. Severson, and I. H. Tombach, 1970: Flight qualification tests performed on air turbulence measuring set AN/AMQ-26. Meteorology Research, Inc., Final Rept. MRI 70-FR-944 to Electronic Systems Div., USAF, Cont. F19628-68-C-0229, p 70.

Hackett, J. F., and J. G. Theisen, 1971: Vortex wake development and aircraft dynamics. In Aircraft Wake Turbulence and its Detection, (Ed. J. H. Olsen, et al.), Plenum Press, 243-263.

Harvey, J. K., and J. E. Fackrell, 1970: Observation of a mechanism causing a trailing contrail vortex to break up. Imperial College, London, AERO Report 70-08.

Kuhn, G. D., and J. N. Nielsen, 1972: Analytical studies of aircraft trailing vortices. AIAA Paper 72-42.

MacCready, P. B., Jr., 1964: Standardization of gustiness values from aircraft. J. Appl. Meteor., 3, 439-449.

MacCready, P. B., Jr., 1966: Operational application of a universal turbulence measuring system. AIAA Paper 66-364.

MacCready, P. B., Jr., 1971: An assessment of dominant mechanisms in vortex-wake decay. In Aircraft Wake Turbulence and its Detection (Ed. J. H. Olsen, et al.), Plenum Press, 289-304.

Olsen, J. H., 1971: Results of trailing vortex studies in a towing tank. In Aircraft Wake Turbulence and its Detection (Ed. J. H. Olsen, et al.,), Plenum Press, 455-472.

Rose, R., and F. W. Dee, 1965: Aircraft vortex wakes and their effects on aircraft. ARC CP No. 795.

Saffman, P. G., 1971: The motion of a vortex pair in an atmosphere of different density. Paper pres. 24th Annual Meeting of the Div. of Fluid Dynamics of the Amer. Phys. Soc.

Scorer, R. S., 1958: Natural Aerodynamics, Pergamon Press, N. Y.

Scorer, R. S., and L. J. Davenport, 1970: Contrails and aircraft downwash. J. Fluid Mech., 43, 451-464.

Smith, T. B., and R. J. Diamond, 1956: Studies of contrails from jet powered aircraft. Meteorology Research, Inc., report to USAF Cambridge Research Center, No. AFCRC-TR-57-254. AD 110 278.

Smith, T. B., and K. M. Beesmer, 1959: Contrail studies for jet aircraft. Meteorology Research, Inc., report to USAF Cambridge Research Center, No. AFCRC-TR-59-251. AD 217 188.

Smith, T. B., and M. A. Wolf, 1963: Vertical diffusion from an elevated line source over a variety of terrains. Meteorology Research, Inc., report, Part A, to Dugway Proving Ground, Cont. DA-42-007-CML-545. AD 418 599.

Smith, T. B., and P. B. MacCready, Jr., 1963: Aircraft wakes and diffusion enhancement. Meteorology Research, Inc., report, Part B, to Dugway Proving Ground. Cont. DA-42-007-CML-545.

Tombach, I. H., 1971: Transport of a vortex wake in a stably stratified atmosphere. In Aircraft Wake Turbulence and its Detection (Ed. J. H. Olsen, et al.), Plenum Press, 41-56.

Tulin, M. P., and J. Shwartz, 1971: The motion of turbulent vortex-pairs in homogeneous and density stratified media. Hydronautics, Inc., Tech. Report 231-15. AD 723 184.

Turner, J. S., 1960: A comparison between buoyant vortex rings and vortex pairs. J. Fluid Mech., 7, 419-432.

Widnall, S. E., D. Bliss, and A. Zalay, 1971: Theoretical and experimental study of the stability of a vortex pair. In Aircraft Wake Turbulence and its Detection (Ed. J. H. Olsen, et al.), Plenum Press, 305-338.

Woodward, B., 1959: The motion in and around isolated thermals. Quart. J. Roy. Meteor. Soc., 85, 144-151.

Reprinted from: AIRCRAFT WAKE TURBULENCE
Edited by John H. Olsen,
Arnold Goldburg and Milton Rogers
Book available from Plenum Publishing Corporation
227 West 17th Street, New York, N. Y. 10011

TRANSPORT OF A VORTEX WAKE IN A STABLY STRATIFIED ATMOSPHERE

I. H. Tombach

Meteorology Research, Inc.

ABSTRACT

Atmospheric stratification affects the downward motion of an aircraft vortex wake and may influence the persistence and stability of the vortex pair configuration. Observations of actual wakes have shown significant variation in the distance to which they descend and in their lifetimes under different degrees of atmospheric stability. This behavior has been modeled analytically in this paper as a pair of infinite vortices in an inviscid, compressible, stably stratified atmosphere with entrainment characterized by a single parameter which is related to the difference between the density in a particular region of the wake and that external to the wake. It has been found that the motion of such a vortex system is governed by a parameter Q which depends on the initial circulation and vortex spacing, on the atmospheric stability, and on the entrainment parameter.

The nature of the transport follows one of two patterns, depending on whether Q is less than or greater than a critical value Q_{crit}. If $Q < Q_{crit}$, the circulation decreases more rapidly than the momentum and the vortices separate as they descend to an equilibrium level. If $Q > Q_{crit}$, the momentum of the vortices decreases more rapidly than the circulation and, after an initial period of slow divergence, the vortices attempt to converge as they descend. In both cases, the

descent takes place in a well-defined characteristic time which depends solely on the atmospheric density gradient.

1. INTRODUCTION

The transport of the trailing vortex wake of an aircraft is frequently modeled by the laminar potential flow solution for a parallel pair of infinite line vortices.[1] This solution indicates that, in the absence of ground effect, the two vortices will descent indefinitely at a constant velocity while maintaining a constant separation. Observations of actual wakes[2,3] have shown, however, that the vortices often stop their descent at some level below the aircraft and then remain near that level until they dissipate. The amount of descent varies from time to time, with atmospheric stability apparently a dominant factor in determining its magnitude. The variation can be quite great. For example, the wake from an aircraft has been observed to descend twenty times as far in the neutrally stable atmosphere over the ocean as in the stable air over land.[4]

A theoretical analysis of the detailed behavior of the wake under these atmospheric conditions is extremely difficult because of the great number of variables involved. Dominant factors involved in a description of the motion include the atmospheric stability, the initial properties of the wake, and the turbulence in the atmosphere and in the wake, which govern the rate at which the wake entrains the surrounding atmosphere and the rate and manner in which the entrained fluid is mixed into the wake. This paper represents an effort to create a simplified approximate model of the dominant effects of atmospheric stability on the transport of a trailing vortex wake, in which only the major aspects of the wake motion are considered and many of the second order effects are ignored. In this model, the wake is represented by a pair of parallel infinite vortices embedded in a nearly elliptical cylinder of accompanying fluid which moves through an inviscid, compressible, stably stratified atmosphere. The effects of entrainment and buoyancy on the circulation are represented by a simplified single parameter model. The approach taken is similar in many respects to that used by Turner.[5]

2. THE EQUATIONS OF MOTION

A schematic portrayal of the vortex pair is shown in Fig. 1. The vorticity is assumed to be concentrated into two contrarotating vortex cores whose diameters are small compared to their separation and each of which has a circulation of magnitude Γ. Fluid within the nearly elliptical cylinder marked by the dashed lines is assumed to be convected together with the vortices, as in the potential flow solution,[6] hence the dashed line is a streamline separating the flow field into two regions: the external atmosphere (whose properties are represented by ρ and T), and the fluid accompanying the vortices (with average properties ρ' and T'). Since the vortices entrain the ambient air, this separation cannot hold rigorously, but it seems a reasonable approximation if the entrainment rate and the descent velocity of the vortex system are sufficiently slow so that, at any particular instant, a near equilibrium state exists and the elliptical shape holds. This assumption of geometric similarity, in which the scale of the wake profile is b, is not valid though for large well mixed wakes in a strongly stable atmosphere, for which a collapse in the vertical extent of the wake, due to gravity, may occur.[7]

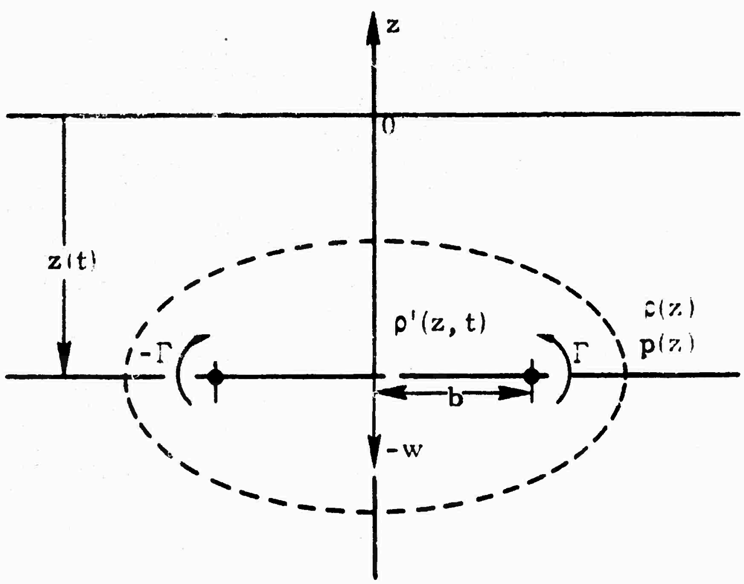

Fig. 1. Schematic cross section of vortex wake

Initially, at t = 0, the fluid properties within the vortex system are the same as those external to it. The properties at the initial level, z = 0, are represented by the subscript $(\ )_o$. It is assumed that the extreme variations encountered for the density are small, i.e., the Boussinesq assumption that $\left|\frac{\rho(z)-\rho_o}{\rho_o}\right| \ll 1$ is made, which holds as long as the descent distance is small compared to the scale height of the atmosphere, viz., as long as $|z| \ll 10$ km.

Using these assumptions, the consequences of which will be discussed later, the equations of motion for the vortex system follow easily. The downward velocity of the entire vortex system is given by

$$w = -\frac{\Gamma}{4\pi b} \tag{1}$$

and the overall vertical momentum of the motion (sometimes called the impulse, and defined as the time integral of all the external forces required to achieve this state of motion[8]) is

$$\begin{aligned} M &= -2\rho'\Gamma b \\ &\approx -2\rho_o\Gamma b \end{aligned} \tag{2}$$

The momentum is affected by the buoyancy which the accompanying fluid acquires, so the momentum conservation equation is

$$\begin{aligned} \frac{dM}{dt} &= g\ V\ (\rho-\rho') \\ &= \rho_o F \end{aligned} \tag{3}$$

where

$$F = g\ V\ \frac{\rho-\rho'}{\rho_o} \tag{4}$$

is a measure of the buoyancy, and the cross-sectional area of the accompanying oval cylinder of fluid is $V = qb^2$. The value of the factor q can be computed numerically for the potential flow solution, and is approximately 11.62.

The mass of fluid in the oval cylinder changes only if there is entrainment of the ambient air. As the cylinder descends, the volume occupied by the accompanying fluid changes due to compressibility, as well as entrainment, hence the mass conservation equation is

$$\frac{d}{dt} (\rho' V) = \rho\left(\frac{dV}{dt} - \frac{gV}{a^2} w\right) \quad (5)$$

where a is the speed of sound in the ambient air. It is assumed here that there is no heat transfer to the vortex system, except for that which is convected along with the entrained mass, so that changes in the cylinder volume would occur adiabatically in the absence of entrainment. The term gVw/a^2 in Eq. (5) is the adiabatic rate of change of volume, which is subtracted from the total rate of volume change to compute the increase in volume due to entrainment.

It is convenient at this point to introduce

$$G = - \frac{g}{\rho_o} \frac{d\rho}{dz} - \frac{g^2}{a_o{}^2} \quad (6)$$

as a measure of the stability of the atmospheric stratification. G is the difference between the actual atmospheric density gradient and the adiabatic one, multiplied by $- g/\rho_o$. Over the range of altitude a wake travels, it is consistent with previous approximations to assume G to be a constant. Positive values of G correspond to stable stratification.

Some manipulation of Eq. (5) gives then the mass conservation equation as

$$\frac{dF}{dt} = - GVw \quad (7)$$

assuming again that density changes are small over the distance traveled.

When the vortex system has acquired buoyancy, the circulation about each vortex is altered by the buoyancy. The circulation equation for inhomogeneous fluids (the Bjerkness equation) is[9]

$$\frac{d\Gamma}{dt} = - \oint_C \frac{1}{\rho} \nabla p \cdot \underline{d\ell} \quad (8)$$

where C is the contour along which the circulation is computed. For the present application, take C as shown in Fig. 2, so that legs 1 through 3 are entirely in the ambient atmosphere and leg 4 bisects the oval along the line of symmetry between the vortices. Then, assuming the density outside the oval to be of an undisturbed

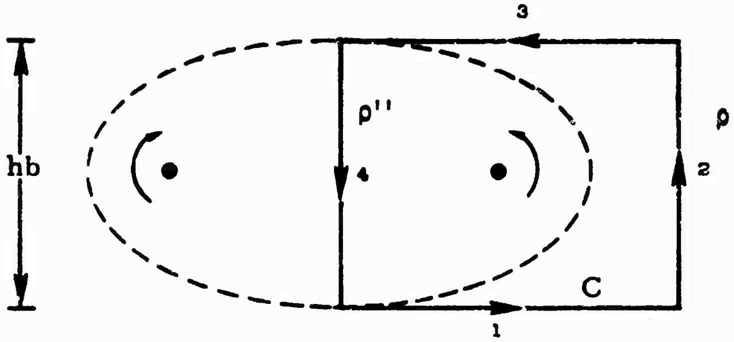

Fig. 2. Circuit used to compute rate of change of circulation

constant value ρ over the distance corresponding to the height of the oval, and the density along leg 4 inside the oval to be ρ'', and noting that $\nabla p = -\rho g$ in the vertical direction, evaluation of the line integral in Eq. (8) gives, taking legs 1 through 4 in order

$$\frac{d\Gamma}{dt} = 0 + \frac{\rho g}{\rho} hb + 0 - \frac{\rho g}{\rho''} hb$$

$$= -\,ghb\,\frac{\rho-\rho''}{\rho''} \tag{9}$$

where hb is the height of the oval. The density ρ'' along the dividing line need not be the same as the average over the whole oval, ρ', and the difference between ρ'' and ρ' will depend on the entrainment rate and the internal mixing rate. Hence the rate of change of circulation depends on the "aspect ratio" of the oval, the buoyancy and entrainment, the internal mixing, and the scale of the vortex system. This change in circulation is assumed to affect the wake as though it took place as a decrease in the circulation of the concentrated vortices, although in actuality the vorticity would be distributed over the volume of the wake.

Since buoyancy will tend to make the upper surface of the oval cylinder unstable while stabilizing the lower surface, and since the descending cylinder is a bluff body, it is likely that most of the entrained mass of ambient fluid will be drawn in at the upper side of the oval. Because of the rotation of the vortices, it will then initially circulate downward near the dividing plane between the two vortices while mixing with the wake fluid. It is useful to interpret the mixing in terms of a length by noting that the density ρ'' along this dividing plane will be formally the same density as that which would be obtained by adiabatic compression of a parcel of ambient air taken from a level some distance Δz above the level of the vortex system. Thus Δz can be considered as a dimension which characterizes the rate of entrainment and the rate at which the entrained air mixes with the fluid already within the cylinder.

Relating $\rho''(z)$ to $\rho(z+\Delta z)$ using the adiabatic density gradient, and $\rho(z)$ to $\rho(z+\Delta z)$ using the actual density gradient, and using the usual density approximation, Eq. (9) can thus be written

$$\frac{d\Gamma}{dt} = - Ghb\Delta z \ . \qquad (10)$$

At this point, it is necessary to assume some element of the entrainment process in order to determine the behavior of Δz. It is instructive to consider some representative ways in which ρ'' could vary as the wake descends. One extreme sample of possible behavior is the case with $\Delta z = 0$, which would occur if the internal mixing was sufficiently weak so that the entrained fluid was still at ambient density along the dividing plane, and thus circulation would remain constant as the wake descended. There would still be some buoyancy though because, although $\Delta z = 0$ implies that ρ'', the density along the dividing plane, will be equal to the local ambient density ρ, it is likely that the mean internal density ρ' will still be less than ρ. If Δz is greater than zero, then there is mixing between the entrained fluid and the buoyant fluid already within the oval and thus ρ'' is less than the ambient density. As will be shown later, an increase in Δz also corresponds to an increased entrainment rate, which would be expected to follow from the increased mixing.

For a realistic case with finite entrainment, it seems valid to assume that, if the heretofore hypothesized geometric similarity of the wake configuration is reasonable, then Δz should probably also scale in the same way as all the other dimensions. Hence, it is assumed that $\Delta z = mb$, where m is an unknown constant. (The vortex half-spacing b is not the only length scale which could be used, but it is probably the dominant one for Δz. If Δz is artificially visualized as the distance above the wake from which the fluid along the dividing plane was supplied, such an assumption seems plausible.) A similar assumption, simplified for an incompressible fluid, was used by Turner[5] and experiments by Woodward[10] with thermals (which are like buoyant entraining vortex rings) seem to provide some experimental substantiation for it.

Using the above assumption and incorporating the constants h and m into one constant s = hm allows Eq. (10) to be written as

$$\frac{d\Gamma}{dt} = - sGb^2 \ . \tag{11}$$

Eqs. (1), (2), (3), (7), and (11) are the five equations which will be solved in the next section for the five unknowns M, F, Γ, b, and w in terms of the initial conditions, the stability of the atmosphere, G, and the parameter s.

3. THE SOLUTION FOR THE MOTION

It is useful to non-dimensionalize all of the variables, so let

$$t = \left(\frac{8\pi}{q}\right)^{1/2} G^{-1/2} \tau \tag{12}$$

$$F = Bf \tag{13}$$

$$M = \rho_0 \left(\frac{8\pi}{q}\right)^{1/2} BG^{-1/2} m \tag{14}$$

$$\Gamma = \frac{1}{2}\left(\frac{8\pi}{q}\right)^{1/2} (3s)^{1/3} B^{2/3} G^{-1/6} \gamma \tag{15}$$

$$b = (3s)^{-1/3} B^{1/3} G^{-1/3} \beta \tag{16}$$

and

$$z = (3s)^{2/3} q^{-1} B^{1/3} G^{-1/3} \zeta \tag{17}$$

where τ, f, m, γ, β, and ζ are the non-dimensional variables corresponding to t, F, M, Γ, b, and z, respectively. The constant B will be chosen later. Note that for τ to be real and meaningful G must be positive and non-zero, i.e., the density gradient must be stable. (Solution for G = 0 will not be considered here.)

In terms of the non-dimensional variables, the equations of motion become

$$\frac{d\zeta}{d\tau} = -\frac{\gamma}{\beta} \tag{18}$$

$$m = \gamma\beta \tag{19}$$

$$\frac{dm}{d\tau} = f \tag{20}$$

$$\frac{df}{d\tau} = -\beta^2 \frac{d\zeta}{d\tau} \tag{21}$$

and

$$\frac{d\gamma}{d\tau} = -\frac{2}{3}\beta^2 \tag{22}$$

The solutions, using the initial conditions $\gamma(\tau = 0) = \gamma_0$, $m(\tau = 0) = m_0$, $\beta(\tau = 0) = \beta_0$, $f(\tau = 0) = 0$, and $\zeta(\tau = 0) = 0$ are easily found to be

$$m = m_0 \cos \tau \tag{23}$$

$$f = - m_0 \sin \tau \tag{24}$$

$$\gamma = m_0^{2/3}\left\{ Q - (\tau + \sin \tau \cos \tau)\right\}^{1/3} \tag{25}$$

$$\beta = - m_0^{1/3} \frac{\cos \tau}{\left\{ Q - (\tau + \sin \tau \cos \tau)\right\}^{1/3}} \tag{26}$$

and

$$\frac{d\zeta}{d\tau} = m_0^{1/3} \frac{\left\{ Q - (\tau + \sin \tau \cos \tau)\right\}^{2/3}}{\cos \tau} \tag{27}$$

where $Q = \gamma_0{}^3/m_0{}^2$. The non-dimensional descent distance ζ is obtained by a numerical integration of Eq. (27). It should be recalled that m_0 is negative for the usual wake.

Although m and f depend only on the time τ, the other variables γ, β, and $d\zeta/d\tau$ depend also on the initial parameter $Q = \gamma_0{}^3/m_0{}^2$. In particular, the solutions differ depending on whether this initial parameter is less than, equal to, or greater than $\pi/2$. If $Q < \pi/2$, the circulation decays to zero before the momentum; if $Q = \pi/2$, the circulation and momentum reach zero simultaneously; and if $Q > \pi/2$, the momentum decays more rapidly than the circulation. Since all the solutions are expressed in terms of some power of m_0, reference to Eqs. (12) through (17) gives the interesting result that B can be chosen arbitrarily.

4. DISCUSSION OF THE MOTION

The solutions given by Eqs. (23) through (27) are plotted in Fig. 3 for a representative value of $Q < \pi/2$, in Fig. 4 for $Q = \pi/2$, and in Fig. 5 for $Q > \pi/2$. Also shown on these figures is the numerically computed curve for the non-dimensional descent ζ.

Some major characteristics of the solution can be obtained directly from the non-dimensionalization. In particular, Eq. (12) shows that the time scale of the motion is proportional to $G^{-1/2}$, hence the greater the

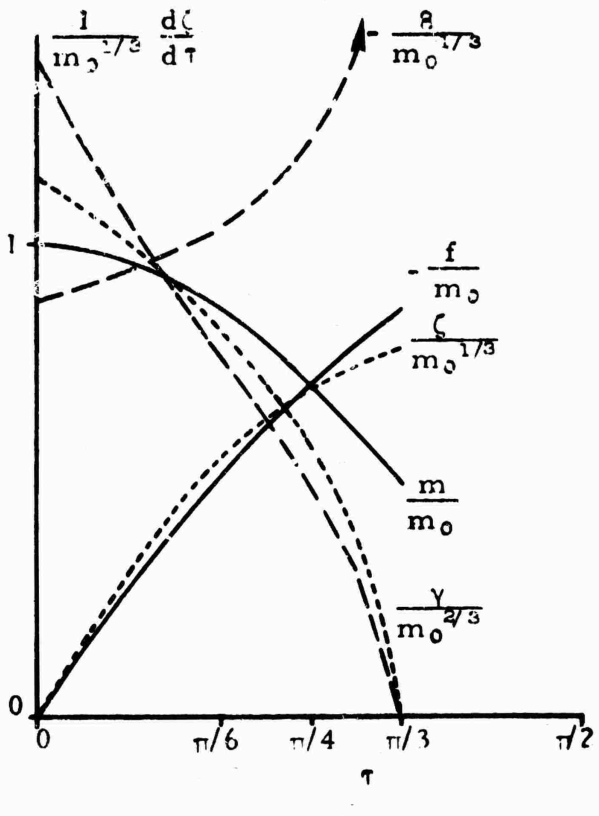

Fig. 3. Solution for Q = 1.48

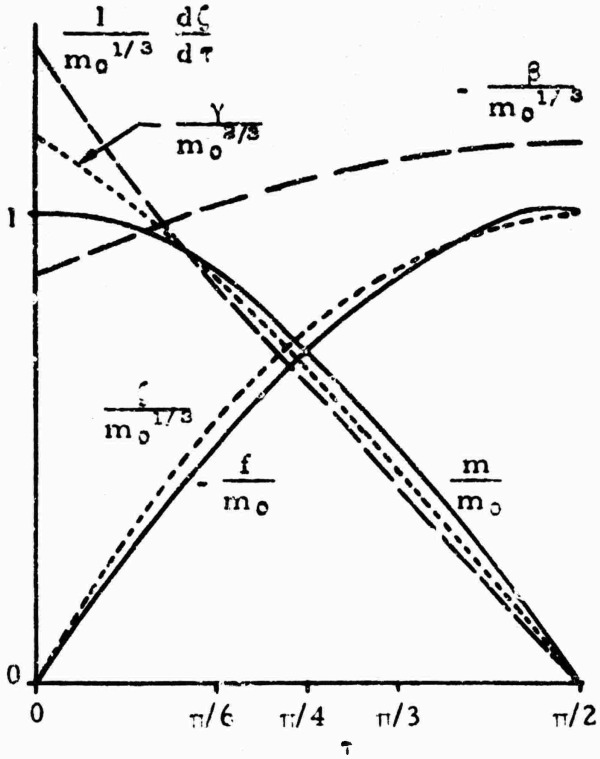

Fig. 4. Solution for Q = π/2

atmospheric stability, the shorter the actual time which is required for the motions shown in Figs. 3, 4, and 5 to take place. Similarly, Eq. (17) indicates that the descent will be less if the stability is greater, which is further reinforced by the decrease in Q as the stability increases. (See Eq. (28) below.)

Interpretation of some aspects of the motion is easier in terms of the physical variables. In particular, the initial condition parameter is

$$Q = \frac{\gamma_0^3}{m_0^3} = \frac{2}{3sG^{1/2}} \left(\frac{q}{8\pi}\right)^{1/2} \frac{\Gamma_0}{b_0^2} \qquad (28)$$

so a decrease in stability will increase Q, as will an increase in initial circulation or a decrease in the initial vortex spacing.

The case with Q < π/2 might be called a "weak vortex" or strong stability case. Here the buoyancy kills the circulation quite rapidly, so that at some time τ < π/2 the circulation becomes zero while m is still

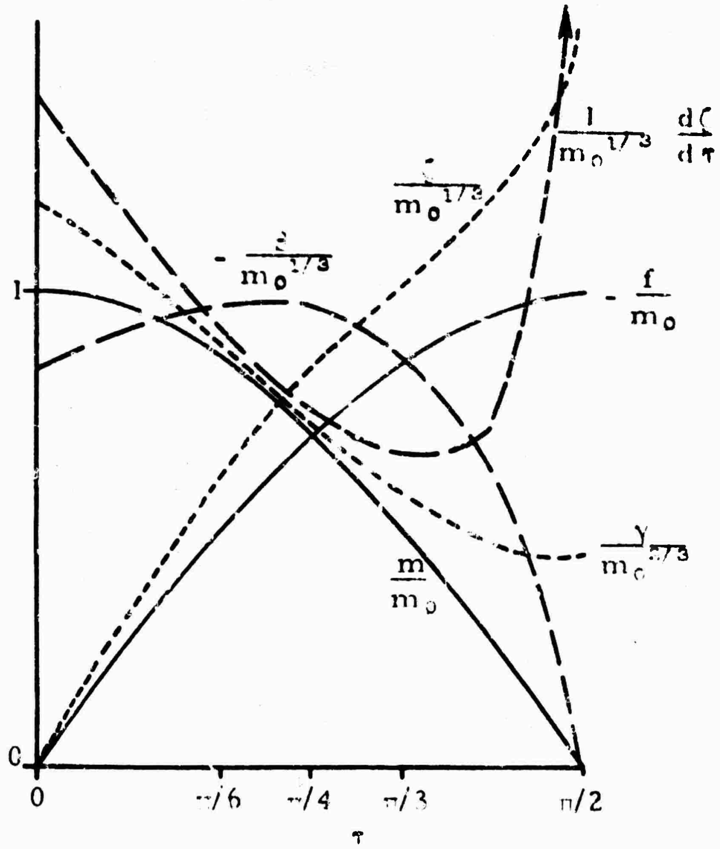

Fig. 5. Solution for Q = 1.66

non-zero. This requires that the spacing between the vortices become very large (at $\tau = \pi/3$ for the example in Fig. 3). Overall, the behavior qualitatively resembles that of a vortex pair in ground effect.

If the initial circulation is increased until $Q = \pi/2$, then the situation shown in Fig. 4 prevails. The circulation and momentum both decay to zero in the same time, at which point the wake is a motionless, buoyant cylinder of scale $b = 4/3\ b_0$. Subsequent solution as the wake buoys upward after $\tau = \pi/2$ is not straightforward since it is not reasonable to assume that s is a constant through the last stages of decay and the start of the buoyancy-created circulation. For times $\tau < \pi/2$, the solution is qualitatively the same as that in Fig. 3, with the circulation, momentum, and velocity decreasing and the buoyancy and separation increasing.

For the strong vortex or weak stability case, in which $Q > \pi/2$, the initial behavior is again the same, as shown in Fig. 5. But, as the momentum decays more rapidly than the circulation, the vortices begin to close together and the velocity of descent begins to increase. In a real wake, although a certain amount of shrinking of the scale is possible since the pressure increases as the wake descends, any substantial decrease in scale would require a loss of fluid from the wake. It is unlikely that such a loss of fluid could take place in an orderly manner, and thus the shrinking portion of the solution is probably unstable and may result in a collapse of the ordered motion.

The rate of entrainment by the vortex system can be calculated directly from the equations of motion, and is best expressed as the rate of change of wake mass per unit distance of descent:

$$-\frac{d}{dz}(\rho' V) = \rho V \left\{ \frac{\rho_o g}{a_o^2} \frac{1}{\rho} - \frac{4\pi F}{\Gamma^2} + \frac{\pi s G}{\rho_o^3} \frac{(-M)^3}{\Gamma^5} \right\} \qquad (29)$$

(Recall that for the descending wake M and z are negative.) Eq. (29) indicates that, for any given set of local wake properties, the entrainment rate increases with increasing s and G, but decreases with increasing F. Hence, overall buoyancy (F) tends to reduce entrainment, possibly as a result of the stabilization of the rotating vortices by the light fluid, while buoyancy between the vortices (s) increases entrainment and acts as a destabilizing influence.

The relationship between increasing s and increasing entrainment, when applied to Eq. (28), shows that increasing values of Q correspond to decreasing entrainment if all other parameters remain fixed. This now helps explain the two distinct characteristics of the solutions for Q less than $\pi/2$ and greater than $\pi/2$. In Fig. 3, with $Q < \pi/2$, the effect of the strong combination of stability and entrainment relative to vortex strength is such as to cause the wake to stop its descent and to grow. In Fig. 5, where $Q > \pi/2$, the weak mixing and entrainment result in buoyancy eventually controlling the vortex motion by decreasing the wake momentum. This results in detrainment of fluid from the oval. (Note that detrainment is possible for $s > 0$ if F/Γ^2 is large enough.)

These aspects of the wake motion are displayed in a different manner in Fig. 6, in which the vortex separation is plotted as a function of the distance of descent.

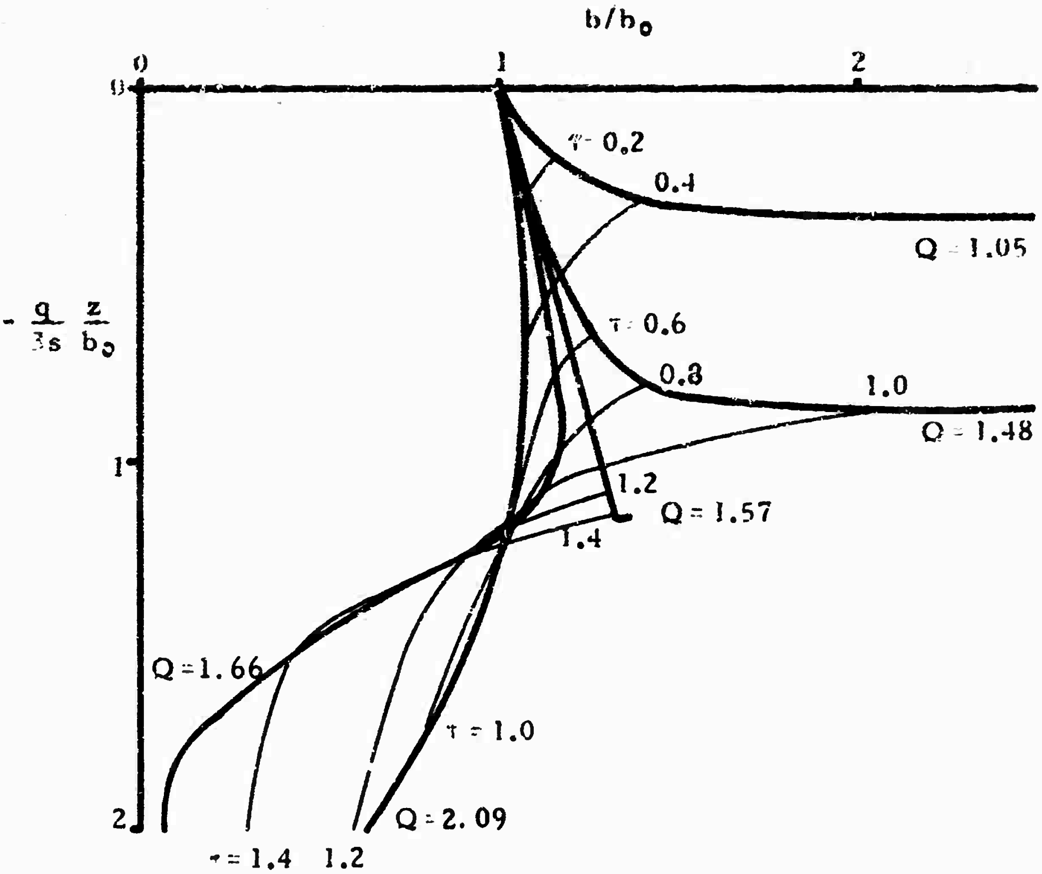

Fig. 6. Variation of vortex spacing with descent distance. The thin lines connect points of equal τ.

The vertical distance scales inversely with s, so that increasing entrainment results in a greater descent due to the decreased buoyancy. Counterbalancing this, increased entrainment manifests itself in greater vortex separation, since Q decreases with increasing s, and consequently in decreased descent velocity and decreased descent. Consideration of increases in stability is easier and the result is always a decreased descent.

For most modern aircraft, ranging from the DC-3 to the Boeing 747, the ratio Γ_0/b_0^2 is about 1 s^{-1}. For a moderately stable atmosphere, $G^{1/2}$ is about 0.02 s^{-1}. The constant q is approximately 12 and s is probably of the order of 10. Insertion of these numbers into

Eq. (28) gives $Q \sim 2$, hence real wakes appear to fall near the range of values of Q considered in Fig. 6. For the same atmospheric conditions, the time $\tau = \pi/2$ over which the motion takes place corresponds to about 100 seconds.

5. CONCLUSIONS

To ascertain the validity of the solutions which have been obtained, it is useful to look again at some of the assumptions which were used in the analysis. It can be shown that the Boussinesq assumption that the overall density differences are small results in approximately correct equations of motion only if the following inequality is satisfied:

$$\frac{w^2}{a_0^2} << \left| \frac{\rho - \rho'}{\rho'} \right| << 1 \quad . \qquad (30)$$

Initially, when the wake is moving downward with no buoyancy, this condition is violated and thus the very start of the motion is modeled incorrectly. This is probably a relatively unimportant error.

It was also assumed that the wake cross-sectional shape is geometrically similar at all times and that the parameter Δz was proportional to the scale of this profile. The similarity assumption is probably valid as long as the wake is not too far from potential flow conditions, in that it is not very buoyant and the entrainment is not too great. The proper approach to use toward entrainment is not clear and experiments such as those performed by Woodward[10] are the only recourse. The assumption used in the present work gives reasonable results but, being coupled to the similarity assumption, it breaks down whenever the similarity does. Consequently, this model is unable to show the expected vertical oscillation of the wake about an equilibrium level.

The obtained solution is thus most accurate for describing the wake descent to the equilibrium level. Since one of the methods by which the aircraft wake decays is due to a breakup of the parallel configuration because of vortex interactions, the determination of the change in vortex spacing gives a clue to the stability of the wake. In particular, one might expect the case in which the vortices try to converge ($Q > \pi/2$) to be particularly unstable and the lifetime of the organized wake to be quite short.

It is apparent that, in the presence of a stable atmospheric density gradient, the transport of the vortex wake is quite different from that predicted by the potential flow solution. The above model suggests some ways in which atmospheric stability and the entrainment mechanism act to influence the overall motion.

Unfortunately, it is not possible to evaluate the validity of the obtained results by comparison with existing experiment. Except for some measurements which are not sufficiently complete to provide the necessary detail,[2,3] the author knows of no published data in which the stability of the atmosphere was measured along with the descent and growth of the wake. Such experimental data are necessary to determine both the validity of the model and to ascertain the value of s. In the absence of detailed data, all that can be said is that the behavior predicted by the model is intuitively reasonable and the numbers presented are of the right magnitude.

ACKNOWLEDGMENT

The author is indebted to the Air Force Office of Scientific Research for support of this research.

REFERENCES

1. Prandtl, L., and O. G. Tietjens, Fundamentals of Hydro- and Aeromechanics. Dover Publications, New York, 1957, pp 209-212.

2. Smith, T. B., and P. B. MacCready, Jr., "Aircraft Wakes and Diffusion Enhancement." Meteorology Research, Inc., Altadena, Calif., Final Report to Dugway Proving Ground, Dugway, Utah, Cont. DA-42-007-CML-545, 1963.

3. Andrews, W. H., "Flight Evaluation of the Wing Vortex Wake Generated by Large Jet Transports." Paper presented at Symp. on Aircraft Wake Turbulence, Seattle, September 1-3, 1970.

4. MacCready, P. B., Jr., "An Assessment of Dominant Mechanisms in Wake Decay." Paper presented at Symp. on Aircraft Wake Turbulence, Seattle, September 1-3, 1970.

5. Turner, J. S., "A Comparison between Buoyant Vortex Rings and Vortex Pairs." J. Fluid Mech., 7 (1960), 419-432.

6. Lamb, Sir Horace, Hydrodynamics. Dover Publications, New York, 1945, pp 221-222.

7. Schooley, A., "Airplane Contrails Related to Vertical Wake Collapse." Bull. Amer. Meteor. Soc., 50 (1969), 719.

8. Lamb, op. cit., pp 161-162.

9. Prandtl, op. cit., pp 194-195.

10. Woodward, B., "The Motion in and around Isolated Thermals." Quart. J. Roy. Meteor. Soc., 85 (1959), 144-151.

ADDENDUM

After the above paper was written, the work of Scorer and Davenport* on the same problem was brought to the author's attention. They solve exactly the same equations of motion, but assume that Γ is a constant (equivalent to Δz or $s = 0$ in the present solution) so their solution is the limiting one for $Q \gg \pi/2$, in which the vortices converge as they descend. They maintain that this configuration is stable up to a certain time (equal to $\tau = 0.66$ in the present paper) because the vorticity generated along the buoyant upper surface is detrained and so no instability is produced in the vortices. (This also justifies the assumed constant circulation.) After this time, according to their model, some of the external fluid and vorticity is mixed into the vortex oval and eventually results in its destabilization and destruction.

*Scorer, R. S., and L. J. Davenport, "Contrails and Aircraft Downwash." J. Fluid Mech., 43 (1970), 451-464.

PRESENTATIONS AND PUBLICATIONS

Two papers related to the research carried out under this contract were presented at the AFOSR/BSRL Symposium on Aircraft Wake Turbulence in Seattle, Washington, on 1-3 September 1970. One paper, presented by Dr. Paul B. MacCready, Jr., and titled "An Assessment of Dominant Mechanisms in Vortex-Wake Decay," was a review of the dominant factors influencing vortex transport and decay, with emphasis on the interaction between the wake and the environment.

The second paper, presented by Dr. Ivar H. Tombach and titled "Transport of a Vortex Wake in a Stably Stratified Atmosphere," presented the wake transport model which was discussed in Section 2 of this report.

Both papers have been published in the proceedings of the symposium, Aircraft Wake Turbulence, edited by John H. Olsen, Arnold Goldburg, and Milton Rogers, and published by Plenum Press, New York, in 1971. A copy of the Tombach paper is included as Appendix A of this report.

The subsequent experimental program and its results have been presented formally and informally at a variety of institutions:

1. California Institute of Technology (Aeronautics Seminar)
2. NASA, Langley Field, Va.
3. AFOSR, Arlington, Va.
4. FAA, Washington, D. C. (invited presentation)
5. DOT Transportation Systems Center, Cambridge, Mass.
6. McDonnell Douglas Corp., Long Beach, Calif. (invited presentation).

These presentations included the showing of an edited selection of motion picture sequences illustrating phenomena of interest and discussions of the experimental data.

An abstract of a proposed paper has been submitted to the American Institute of Aeronautics and Astronautics for their consideration for presentation at the AIAA 11th Aerospace Sciences Meeting in January 1972. This paper will discuss the results of this research program.